

1
2
3
4
5
6
7
8
9
10
11
12
13
14
15
16
17
18
19
20
21
22
23
24
25
26
27
28
29
30
31
32
33
34

Supplementary Information for

Small-molecule targeting of GPCR-independent non-canonical G protein signaling inhibits cancer progression

Jingyi Zhao^{1†}, Vincent DiGiacomo^{1†*}, Mariola Ferreras-Gutierrez², Shiva Dastjerdi³, Alain Ibáñez de Opakua⁴, Jong-Chan Park¹, Alex Luebbbers¹, Qingyan Chen¹, Aaron Beeler³, Francisco J Blanco² and Mikel Garcia-Marcos^{1*}

¹*Department of Biochemistry, Boston University School of Medicine, Boston, MA 02118, USA.*

²*Centro de Investigaciones Biológicas CIB-CSIC, Madrid, Spain*

³*Department of Chemistry, Boston University, Boston, MA 02115, USA.*

⁴*German Center for Neurodegenerative Diseases, DZNE, Göttingen, Germany.*

*Corresponding author(s): Mikel Garcia-Marcos (mgm1@bu.edu) and Vincent DiGiacomo (Vincent.DiGiacomo@gmail.com)

†Contributed equally to this work

‡Current address: Jorna Therapeutics, Cambridge, MA 02139, USA.

Supplementary information includes 8 figures and 1 table

Materials and Methods

Figs. S1 to S9

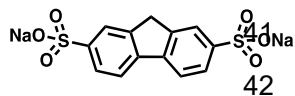
Table S1

Supplemental references

35 **MATERIALS and METHODS**36 **Synthesis of chemical compounds**

37 IGGi-11 (4'-((9H-fluorene-2,7-disulfonyl)bis(methylazanediy))dibutyric acid) was purchased from
 38 Chembridge or Sigma (R693073), or synthesized as follows. Synthesis of IGGi-11me from IGGi-11 is also
 39 described below.

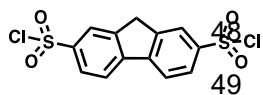
40



Chlorosulfonic acid (1 ml, 20 mmol, 3 equiv) was added dropwise at 0 °C to a stirred
 solution of fluorene (1 g, 6 mmol, 1 equiv) in acetic acid (10 ml, 0.6 M). The reaction

43 mixture was refluxed for 2 h, cooled and poured into a saturated aqueous solution of NaCl (10 ml) containing
 44 NaOH (600 mg, 2.5 equiv) to obtain a yellow precipitate (1.9 g, 90%). The precipitate was washed three times
 45 with a saturated solution of NaCl, filtered and dried overnight at 60 °C to give disodium 9H-fluorene-2,7-
 46 disulfonate as an off-white solid (1.9 g, 90%).

47



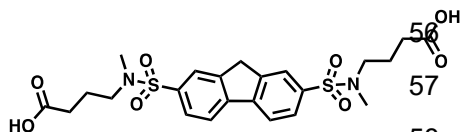
Sodium 9H-fluorene-2,7-disulfonate (2g, 5 mmol, 1 equiv), PCl₅ (3g, 20 mmol, 3 equiv)
 and POCl₃ (6 mL, 60 mmol, 12 equiv) were heated to reflux for 16 h. POCl₃ was

50 removed by distillation before water was added slowly and the mixture was sonicated to break up the
 51 aggregates. The solid obtained was filtered to obtain 9H-fluorene-2,7-disulfonyl dichloride as a brown solid
 52 (1.87g, 100%).

53 **¹H NMR (500 MHz, CDCl₃)** δ 8.31 (s, 2H), 8.18 (d, *J* = 7.9 Hz, 2H), 8.11 (d, *J* = 8.2 Hz, 2H), 4.21 (s, 2H).

54 **¹³C NMR (126 MHz, CDCl₃)** δ 145.62, 145.41, 144.23, 126.77, 124.11, 122.26, 37.30.

55



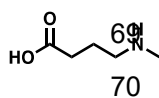
4-(Methylamino)butanoic acid (19 mg, 0.17 mmol, 2 equiv) and
 DIPEA (43 μl, 0.25 mmol, 3 equiv) were added to a 1-dram vial
 containing 9H-fluorene-2,7-disulfonyl dichloride (30 mg, 0.08 mmol,
 1 equiv) in DMA (1 mL). The mixture was stirred at 23 °C for 12 h until the consumption of the starting material

59 was observed by TLC (DCM: MeOH, 97:3). The mixture was then quenched with 1M HCl (1.2 ml) and was
 60 extracted three times with DCM and washed three times with brine. The crude was dried over Na₂SO₄ and
 61 the solvent was evaporated *in vacuo* and purified by column chromatography (DCM: MeOH, 97:3) to afford
 62 a white solid (35 mg, 81%, >95% purity).

64 **¹H NMR (500 MHz, CD₃OD)** δ 8.15 (d, *J* = 8.1 Hz, 2H), 8.07 (s, 2H), 7.88 (dd, *J* = 8.1, 1.7 Hz, 2H), 4.16 (s,
 65 2H), 3.10 (t, *J* = 6.9 Hz, 4H), 2.77 (s, 6H), 2.37 (t, *J* = 7.2 Hz, 4H), 1.83 (p, *J* = 7.1 Hz, 4H).

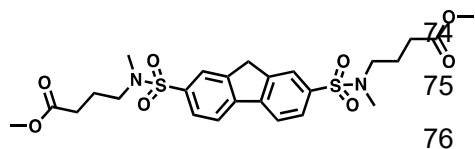
66 **¹³C NMR (126 MHz, (CD₃)₂SO)** δ 173.22, 145.27, 143.94, 137.22, 126.57, 124.40, 121.33, 49.41, 36.91,
 67 34.34, 29.76, 22.64.

68 **HR-MS (*m/z*):** [C₂₃H₂₈N₂O₈S₂+H]⁺ calculated: 525.1365; found: 525.1355 (+1.9043 ppm).



4-(Methylamino)butanoic acid used in the reaction above was synthesized as follows:
70 hydrochloric acid (7 ml, 7.2 M) was added to 1-methylpyrrolidin-2-one (5 g, 50 mmol, 1 equiv)

71 and the mixture was heated to reflux for 16 h. The HCl was evaporated in Genevac and the crude material
72 was purified by column chromatography (DCM: 10% NH₄OH/MeOH, 90:10) to afford the final product as an
73 off-white solid (4 g, 70%).



Thionyl chloride (5.7 μl, 79 μmol, 2.06 equiv) was added to a
74 solution of 4,4'-((9H-fluorene-2,7-
76 disulfonyl)bis(methylazanediyl))dibutyric acid (20 mg, 38 μmol, 1

77 equiv) in MeOH (1 ml) at 0 °C, and the solution stirred for 1.5 h. The solvent was evaporated *in vacuo* to
78 afford the final product **IGG-11me** as a white solid with no further purification (21.5 mg, quantitative, >95%
79 purity).

80 **¹H NMR (400 MHz, CDCl₃)** δ 8.00 (s, 2H), 7.96 (d, *J* = 8.1 Hz, 2H), 7.85 (d, *J* = 8.0 Hz, 2H), 4.07 (s, 2H),
81 3.68 (s, 6H), 3.10 (t, *J* = 6.8 Hz, 4H), 2.77 (s, 6H), 2.44 (t, *J* = 7.2 Hz, 4H), 1.88 (p, *J* = 7.1 Hz, 4H).

82 **¹³C NMR (101 MHz, CDCl₃)** δ 126.74, 124.29, 121.20, 53.77, 51.69, 49.40, 42.04, 34.76, 30.61, 22.69, 18.63,
83 17.37, 12.02.

84 **HR-MS (*m/z*):** [C₂₅H₃₂N₂O₈S₂+H]⁺ calculated: 553.1678; found: 553.1688 (+1.8078 ppm).

85 All ¹H NMR spectra were recorded at 400 or 500 MHz at ambient temperature with CDCl₃, CD₃OD,
86 DMSO (d₆) or D₂O as the solvent. Chemical shifts are recorded in parts per million (ppm) relative to CDCl₃
87 (¹H, δ 7.26; ¹³C, δ 77.1), CD₃OD (¹H, δ 3.31; ¹³C, δ 49.0), (CD₃)₂SO (¹H, δ 2.50; ¹³C, δ 39.5) or D₂O (¹H,
88 δ 4.79). Analytical LC-MS was performed on a Waters Acquity UPLC (Ultra Performance Liquid
89 Chromatography (Waters MassLynx Version 4.1) with a Binary solvent manager, SQ mass spectrometer,
90 Water 2996 PDA (PhotoDiode Array) detector, and ELSD (Evaporative Light Scattering Detector).

91

92 Reconstitution of compound solutions

93 Powder stocks of IGGi-11 were resuspended in DMSO at a final concentration of 100 mM and directly
94 diluted in aqueous solutions up to a 1 mM concentration for experiments. Powder stocks of IGGi-11me were
95 resuspended in DMSO at a final concentration of 40 mM and diluted in aqueous solutions for biological
96 experiments as described next. One-thousand and five hundred μl of cell culture media were added to a 15
97 ml conical tube with 3.75 μl of 40 mM IGGi-11me at the bottom, and pipetted up and down 8-10 times for
98 mixing. This solution was incubated at room temperature for 10 min in a sonicated bath (EMERSON, Branson
99 Bransonic® CPXH Digital Bath 1800). This solution (100 μM) was used to make serial dilutions as needed.
100 Cell media was replaced by IGGi-11me media for compound treatments.

101 The sources and structures of all other "IGGi" compounds (69 including IGGi-11) are presented in **Table**
102 **S1**. All these compounds were resuspended in DMSO at a final concentration of 40 mM.

103

104 **Plasmids**

105 *E. coli* expression plasmids encoding His-tagged rat Gai3 (rat His-Gai3; pET28b-rGai3), His-tagged
106 human Gai3 (human His-Gai3; pET24d-hGai3), His-tagged rat Gai2 (rat His-Gai2; pET28b-rGai2), His-
107 tagged human Gai1 (human His-Gai1; pPro-Gai1), GST-tagged rat Gai3 (GST-Gai3; pGEX-4T-1-GST-Gai3),
108 His-tagged human GIV-CT (His-GIV-CT (aa 1660-1870); pET28b-hGIV (1660-1870)), and GST-tagged
109 human GST-GIV (1671-1755; pGEX-4T-1 hGIV (1671-1755)) have been described previously (1-7). Plasmids
110 encoding His-tagged RGS4 (His-RGS4, pLIC-His-RGS4), and GST-tagged RGS4 (GST-RGS4, pLIC-GST-
111 RGS4), were generated using a ligation independent cloning (LIC) procedure (8). This procedure was used
112 to insert the sequence encoding human RGS4 into pLIC-His or pLIC-GST vectors kindly provided by J.
113 Sondek (UNC-Chapel Hill, NC) (9). The plasmid encoding His-tagged bovine Gas (pHis6-Gas) was kindly
114 provided by N. Artemyev (University of Iowa). The plasmid for producing myristoylated rat Gai1 used in
115 adenylyl cyclase experiments was generated by amplifying the sequence of Gai1 with an internal His-tag in
116 the b/c loop from a pQE-Gai1H6 plasmid provided by C. Dressauer (University of Texas Health Science
117 Center at Houston, TX) and inserting it in the NdeI/BglII sites of pLIC-His using Gibson assembly (pLIC-
118 int6xHis). The pbb131 plasmid encoding N-myristoyltransferase (NMT) (pbb131-NMT) was a gift from M.
119 Linder (Cornell University) (10). All point mutations were generated using QuikChange II (Agilent, #200523).
120 Mammalian expression plasmids encoding the BRET acceptor Venus-tagged G β γ (pcDNA3.1-Venus[1-155]-
121 G γ ₂[VN-G γ ₂] and pcDNA3.1-Venus[155-239]-G β ₁[VC-G β ₁]) or untagged G β γ (human G β ₁; pcDNA3.1-G β ₁,
122 and human G γ ₂; pcDNA3.1-G γ ₂) were kindly provided by N. Lambert (Augusta University, Augusta, GA) (11,
123 12), and the plasmid encoding bovine GRK3ct (aa 495–688) fused to nanoluciferase and a membrane
124 anchoring sequence, “mas” (mas-GRRK3ct-Nluc; pcDNA3.1-masGRK3ct-NanoLuc) was a kind gift from K.
125 Martemyanov (Scripps Research Institute, Jupiter, FL) (13). The plasmids encoding untagged rat Gai3
126 (pcDNA3-Gai3) and untagged rat Gao (pcDNA3-Gao) have been described previously (14, 15). The plasmid
127 encoding Gaq-HA (mouse, pcDNA3-Gaq-HA, internally tagged) was kindly provided by P. Wedegaertner
128 (Thomas Jefferson University) (16). The plasmids encoding human G α 13 (pcDNA3.1-G α 13 internally EE-
129 tagged; cat#GNA130EI00) or human M3R (pcDNA3.1-3xHA-M3R; cat#MAR030TN00) were obtained from
130 the cDNA Resource Center at Bloomsburg University. The plasmid encoding rat α _{2A}-AR (pcDNA3- α _{2A/D}-AR)
131 (17) was provided by J. Blumer (Medical University of South Carolina, SC), and the plasmid for PAR1 (18)
132 was obtained from Addgene (pBJ-FLAG-hPAR1 #53226). pcDNA3.1(+)-GABA_BR1a and pcDNA3.1(+)-
133 GABA_BR2 were a gift from Paul Slessinger, Mount Sinai NY. The plasmid encoding rat Gai3 with citrine variant
134 of YFP inserted in the ab/ac loop of Gai3 (pcDNA3.1-Gai3-YFP (b/c loop) has been described previously
135 (19). The plasmid encoding human adenylyl cyclase 5 (pcDNA3.1-YFP-hAC5) was a kind gift from C.
136 Dessauer (University of Texas Health Science Center at Houston, TX) (20). The plasmids encoding GIV or
137 control shRNA sequences (pLKO.1-puro-GIV shRNA2, AAGAAGGCTTAGGCAGGAATT; pLKO.1-puro-scr,

138 GGATTGAGATCAGAAGATAGC) have been described previously (25). The lentiviral plasmid encoding myc-
139 tagged firefly luciferase (pLVX-fluc2-myc-IRES-Hyg) was generated in two steps. First, firefly luciferase (fluc2)
140 was amplified by PCR from pGL4.33 (Promega, cat# E1340) and inserted into the NheI/KpnI of pcDNA3.1(+)
141 to generate pcDNA3.1-fluc2-myc. Then, the fluc2-myc cassette was PCR amplified and inserted into the
142 XhoI/BamHI sites of pLVX-IRES-Hyg (Clontech, cat# 632185) by Gibson assembly to generate pLVX-fluc2-
143 myc IRES-Hyg. Lentiviral packaging plasmids were pSPAX2 (Addgene #12260) and pMD2.G (Addgene
144 #12259). The Glosensor 22-F plasmid (21) was from Promega (cat# E2301).

145 **Protein purification and peptide synthesis**

146 Purification of rat His-Gai3, human His-Gai3, rat His-Gai2, human His-Gai1, human His-GIV-CT (aa
147 1660-1870), human His-RGS4, rat GST-Gai3, human GST-GIV (aa 1671-1755), or human GST-RGS4
148 proteins was carried out as described previously (2, 3) with minor modifications. Briefly, protein expression
149 was induced in BL21(DE3) *E. coli* cells transformed with the appropriate plasmids by overnight incubation
150 with 1 mM isopropyl- β -D-1-thio-galactopyranoside (IPTG) at 23 °C, except for rat His-Gai3 used in the high-
151 throughput fluorescence polarization experiments, which was induced overnight at 23 °C using the Studier's
152 autoinduction method (22). Bacteria pelleted from 1 liter of culture were resuspended in 25 mL of lysis buffer
153 (50 mM NaH₂PO₄, 300 mM NaCl, 10 mM imidazole, 1% (v:v) Triton X-100, 1 μ M Leupeptin, 2.5 μ M Pepstatin,
154 0.2 μ M Aprotinin, 1 mM PMSF, pH 7.4). For G-protein preparation, the buffer was supplemented with 25 μ M
155 GDP and 5 mM MgCl₂. After sonication (four cycles, with pulses lasting 20 s/cycle, and with 1 min interval
156 between cycles to prevent heating), lysates were centrifuged at 12,000 \times g for 20 min at 4 °C. Solubilized
157 proteins were affinity purified on either HisPur Cobalt resin (ThermoFisher cat#89964) for His-tagged proteins
158 or Glutathione Agarose resin (Pierce 16100) for GST-tagged proteins, and eluted with lysis buffer
159 supplemented with 250 mM imidazole or with 50 mM Tris-HCl, 100 mM NaCl, 30 mM reduced glutathione
160 (pH 8), respectively. Eluted proteins were dialyzed overnight at 4°C against PBS, except for G-proteins, which
161 were buffer exchanged to 20 mM Tris-HCl, 20 mM NaCl, 1 mM MgCl₂, 1 mM DTT, 10 μ M GDP, 5% (v/v)
162 glycerol (pH 7.4) on an FPLC system using a HiTrap Desalting column (GE Healthcare cat# 17-1408-01).
163 For human His-Gai3 used in isothermal titration calorimetry experiments, buffer exchange was to 10 mM
164 HEPES, 10 mM MgCl₂, 1 mM TCEP, 300 μ M GDP (pH 7) using the same desalting column. His-tag-cleaved
165 human Gai3 used for nuclear magnetic resonance experiments (2), bovine His-Gas (23), and myristoylated
166 rat Gai1 with an internal His-tag (24) were purified exactly as in the indicated references. All protein
167 preparations were aliquoted and stored at -80 °C. Fluorescently (FITC) labeled peptides corresponding to
168 human GIV (aa 1671-1701, KTGSPGSEVVTLQQFLEESNKLTSSVQIKSSS), RGS12 GoLoco motif (aa 1185-
169 1221, DEAEFFELISKAQSNRADDQRGLLRKEDLVLPFLR, R12 GL), or the synthetic sequence KB-1753
170 (SSRGYYHGIWVGEEGRLSR) were synthesized and purified exactly as described previously (2, 3, 25),
171 dissolved in DMSO, and stored in aliquots at -80 °C.

172

173 High-throughput screen by fluorescence polarization

174 This screen was conducted at the ICCB-Longwood Screening Facility at Harvard Medical School with a
175 collection of ~200,000 compounds from commercial and academic sources. The principle of the assay is
176 based on monitoring binding of a GIV-derived peptide to Gai3, which has been previously shown to
177 recapitulate the properties the native GIV-Gai3 interaction (2, 3). Experimental wells of 384-well assay plates
178 (black ProxiPlate F-Plus, Perkin Elmer cat# 6008269) were pre-filled with FITC-GIV (aa 1671-1701) peptide
179 in a 10 μ l volume of assay buffer (50 mM Tris, 100 mM NaCl, 10 mM MgCl₂, 5 mM EDTA, 0.4% (v:v) NP-40,
180 30 μ M GDP, 1 mM DTT, pH 7.4) using a Multidrop Combi liquid handler (Thermo). Plates were centrifuged at
181 1000xg for 2 minutes to eliminate bubbling on the surface, and 100 nl of experimental compound (in 100%
182 DMSO) was pin-transferred into individual wells in two replicate plates using a D-TRAN XM3106-31 PN robot
183 (Seiko). After pin-transfer, 5 μ l of rat His-Gai3 was added to each well using a Multidrop Combi liquid handler
184 (Thermo), and assay plates were shaken at low speed for 5 seconds. Plates were centrifuged at 1000xg for
185 2 minutes and shaken for 10 seconds prior to an incubation of 90 minutes at room temperature. The final
186 concentrations of assay components were 25 nM for FITC-GIV and 1 μ M for His-Gai3. The typical final
187 compound concentration was approximately 30 μ g/ml, with a final concentration of DMSO per well of 0.67%
188 (v:v). Fluorescence polarization (FP) signal was measured with an EnVision Multilabel 2103 plate reader
189 (PerkinElmer) using a D505fp/D535 dual mirror (Ex 480 nm / Em 535 nm filters, P and S channels). Each
190 plate contained 16 negative control wells containing only 0.67% DMSO without test compound and 16
191 positive control wells containing 30 μ M AlCl₃ and 10 mM NaF (to generate the AlF₄⁻ species that completely
192 disrupts the GIV-Gai3 interaction in this assay format (3)). Negative and positive controls were used to
193 normalize the FP signals to 100% and 0% GIV-Gai3 binding, respectively. Compounds reducing binding 15%
194 or more were considered hits (~580 compounds). Hits were re-tested in this assay format using the same
195 procedure and in an AlphaScreen® assay described below, substituting a D300e liquid dispenser (Hewlett
196 Packard) for compound addition (200 nl). Results of the screen were deposited in PubChem (AID: 1224905).

197

198 AlphaScreen® assay

199 As an approach orthogonal to monitoring the GIV-Gai interaction by fluorescence polarization, we
200 implemented a previously established AlphaScreen® assay. This chemiluminescent assay operates at
201 wavelengths different from those used in the fluorescence polarization assay to monitor the association
202 between Gai3 and a fragment of GIV that recapitulates the binding properties of the full-length protein (2, 3,
203 26). For AlphaScreen® experiments in high-throughput screening format, 200 nl of experimental compounds
204 (“cherry-picked” from the original libraries) diluted in DMSO were added to individual wells of 384-well plates
205 (white ProxiPlate F-Plus, Perkin Elmer cat#6008280) containing 5 μ l of His-GIV-CT (aa 1660-1870) diluted
206 in assay buffer (50 mM Tris, 100 mM NaCl, 5 mM MgCl₂, 0.4% (v:v) NP-40, 50 μ M GDP, pH 7.4). Five μ L of

207 GST-Gai3 diluted in assay buffer were added to each well, and plates were centrifuged at 1000xg for 2
208 minutes, shaken for 10 seconds, and incubated for 90 minutes at room temperature to allow for GIV-Gai3
209 complex formation. Next, 5 μ L of a suspension of AlphaScreen Nickel-chelate donor beads (Perkin Elmer,
210 cat#AS101) and AlphaLISA Glutathione acceptor beads (Perkin Elmer, Cat#AL109) diluted in assay buffer
211 were added to each well. Multidrop Combi liquid handlers (Thermo) were used for dispensing all buffers and
212 reagents, except for compounds, which were delivered using a D300e liquid dispenser (Hewlett Packard).
213 Each compound was tested in triplicate, and the final concentrations of components were as follows: 50-100
214 μ M for compounds (fixed 200 nl volume of library stocks), 75 nM each of His-GIV-CT and GST-Gai3, 10 μ g/ml
215 for AlphaScreen Nickel-chelate donor beads, and 5 μ g/ml for AlphaLISA Glutathione acceptor beads. The
216 final concentration of DMSO was 1% (v:v). Controls included in each run consisted of no compound, DMSO-
217 only negative controls, and AlF_4^- added with His-GIV-CT to disrupt the GIV-Gai3 interaction (3) as positive
218 controls (50 μ M AlCl_3 , 10 mM NaF final concentrations). Signals were read with an EnVision Multilabel 2103
219 plate reader (PerkinElmer) using the AlphaScreen[®]-rated D640as mirror and M570w emission filter (570 \pm
220 50 nm), and normalized to negative (100%) and positive (0%) controls. Compounds reducing the
221 AlphaScreen[®] signal 35% or more compared to negative controls (DMSO) were considered positive hits.
222 Re-testing of freshly purchased compounds was carried out as above but in the presence of different doses
223 of compound (0.05-100 μ M).

224

225 **Triage of hit compounds**

226 Compounds that were deemed hits from both the fluorescence polarization and the AlphaScreen[®]
227 assays were manually evaluated for known pan assay interference (PAINS) moieties and other electrophilic
228 properties that would result in undesired promiscuity. We further excluded compounds with more stringent
229 criteria after applying computational filters to screen for additional PAINS and problematic chemical groups
230 (27, 28).

231

232 **Cell culture and establishment of cell lines**

233 MDA-MB-231 (ATCC #HTB-26), MCF-7 (ATCC #HTB-22), Hs-578T (ATCC #HTB-126), BT-549 (ATCC
234 #HTB-122), MDA-MB-436 (ATCC #HTB-130), MDA-MB-157 (ATCC #HTB-24), T47-D (ATCC #HTB-133),
235 MDA-MB-453 (ATCC #HTB-131), HeLa (ATCC #CCL-2), and HEK293T (ATCC #CRL3216) cells were
236 maintained at 37 $^{\circ}$ C with 5% CO_2 in DMEM (Gibco cat#11-965-118) supplemented with 10% (v:v) fetal bovine
237 serum (FBS), 100 U/ml penicillin, 100 μ g/ml streptomycin, and 2 mM L-glutamine. The medium for some of
238 these cell lines was supplemented as follows: Hs-578T, 0.01 mg/ml insulin; BT-549, 0.002 mg/ml insulin;
239 MDA-MB-436, 0.002 mg/ml insulin; T47-D, 0.002 mg/ml insulin. MCF-10A cells (ATCC #CRL-10317) were
240 maintained in MEGM (Lonza cat#CC3150) supplemented with components of the SingleQuot supplement kit
241 (Lonza cat#C4136) and 100 ng/mL cholera toxin (List Biological Laboratories #100B). The FBS used for all

242 cell lines was from Gibco (Cat# 26140-079), except for HEK293T cells, which were grown in FBS from
243 HyClone (Cat# SH30072.03). MDA-MB-231 stably expressing firefly luciferase were generated by lentiviral
244 transduction followed by antibiotic selection.

245 Lentiviral particles were produced by transfection of HEK293T cells using polyethylenimine (PEI;
246 Polysciences, Inc; #23966, 1 mg/ml solution reconstituted in water). Four hundred thousand cells were
247 seeded per well of a 6-well plate and cotransfected the next day with lentiviral plasmid of interest (1.8 µg)
248 and packaging plasmids psPAX2 (1.2 µg) and pMD2.G (0.75 µg). Plasmid DNA was added to 200 µl of fresh
249 DMEM without serum and mixed with 7.5 µl of PEI reagent by vortexing for 2 seconds. Tubes were incubated
250 at room temperature for 15 min before adding to cells. Six hours after transfection, the media was changed
251 to DMEM with 10% FBS. Lentivirus-containing media were collected 24 hr and 48 hr after transfection and
252 combined together, centrifuged at 1500xg for 5 min, and filtered through a 0.45-µm surfactant-free cellulose
253 acetate (SFCA) membrane (Corning, cat#431220). MDA-MB-231 cells were seeded on 6-well plates
254 (200,000 cells per well). The day after seeding, cells were transduced by a 48 hr incubation with 2 ml of a 1:1
255 mix of lentivirus-containing supernatants described above mixed with fresh complete media and
256 supplemented with 6 µg/ml of polybrene. Cells were transferred to a 10-cm plate and selection with 250 µg/ml
257 hygromycin (GoldBiotechnnology, cat#H-270-5) started the day after. All surviving clones were pooled and
258 maintained in the presence of 250 µg/ml hygromycin.

259 The generation of MDA-MB-231 and HeLa cells stably expressing GIV shRNA or a control shRNA (has
260 been described previously (29). These cells were maintained in their culture medium supplemented with 1
261 µg/ml puromycin (GoldBiotechnnology, cat#P-600-1). HeLa cells stably expressing the biosensors Gai*
262 BERKY3 or Gβγ-BERKY3 have also been described previously (30), and were maintained in their culture
263 medium supplemented with 100 µg/ml hygromycin.

264

265 **Tumor cell migration assay**

266 Cell migration was evaluated using a modified Boyden chamber assay. MDA-MB-231, MCF-7, Hs-578T,
267 BT-549, or HeLa cells were grown to approximately 70% confluency in a 10 cm² culture plate. Cells were
268 washed 3 times with warm citric saline solution (135 mM KCl, 15 mM Sodium Citrate, pH 7.2) and detached
269 by incubation at 37 °C for 10 min in the same citric saline solution. Detached cells were washed with 15 ml
270 medium supplemented with 0.2% FBS three times by cycles of centrifugation (300xg, 3 minutes), aspiration
271 and resuspension. Cells were seeded into the top chamber of each well of a 96-well 8 µm polyester transwell
272 migration plate (Corning cat#3374) in a 40 µl volume of medium supplemented with 0.2% FBS. Forty µl of
273 the same medium (0.2% FBS) containing compounds at 2X of the final concentration indicated in the figures
274 or figure legends were added to the top chamber of the wells and incubated for 1 hour at room temperature.
275 After this serum-starved preincubation with compound, 250 µl of medium supplemented with 10% FBS was
276 added to the bottom chamber to create the chemotactic gradient. The concentration of compound in the

277 bottom chamber was matched to that in the upper chamber, and the concentration of DMSO was maintained
278 constant at 0.5% (v:v) across all conditions. Medium without FBS in the bottom chamber was used a negative
279 control for migration. The initial number of cells seeded per well and the time of incubation at 37 °C in 5%
280 CO₂ to allow the migration of cells was as follows: MDA-MB-231, 25,000 cells for 6 hours; MCF-7, 60,000
281 cells for 18 hours; Hs-578T, 25,000 cells for 16 hours; BT-549, 25,000 cells for 16 hours; HeLa, 25,000 cells
282 for 16 hours. Following the migration period, the top chamber was cleared of non-migratory cells using a
283 cotton swab and medium was aspirated with gentle vacuum. The top chamber was then moved to a receiver
284 plate containing warm PBS (250 µl) to wash the migrated cells on the bottom of the membrane. Fifty µl of
285 PBS was added to the top chamber before doing a second clean with a cotton swab. The PBS in the top
286 chamber was aspirated by vacuum before the chamber was moved to a new receiver plate containing
287 warmed 125 µl of a trypsin solution (Corning, cat # 25-053-C1). To detach the migratory cells from the bottom
288 of the membrane, plates were incubated at 37 °C for 12 minutes, rocked for 5 minutes at room temperature,
289 and tapped on each side. Trypsinized cells were rapidly transferred to a new white, opaque-bottom 96-well
290 plate (Opti-Plate, Perkin Elmer, cat# 6005290) and mixed with an equal volume of CellTiterGlo (Promega,
291 cat# G7570) diluted 1:3 in 10% FBS medium to estimate cell abundance. The mixture was shaken for 2
292 minutes and incubated for 10 minutes at room temperature before reading total luminescence in a Biotek
293 Synergy H1 plate reader. Luminescent counts in the condition without FBS in the bottom chamber was
294 subtracted from all conditions, and the resulting counts were normalized to counts in the DMSO-only control
295 (100%) as a measure of migration. In compound dose dependence experiments, values of 3 technical
296 replicates (wells) were averaged in each independent experiment.

297 For SDF-1 α mediated cell migration assay, MDA-MB-231 cells detached by warm citric saline buffer as
298 described above were washed three times with 15 ml medium without serum by cycles of centrifugation
299 (300xg, 3 minutes), aspiration and resuspension. Twenty-five thousand cells were seeded on the top chamber
300 of each well of a 96-well 8 µm polyester transwell migration plate (Corning cat#3374) in a 40 µl volume of
301 medium without serum. Forty µl of the same medium (no serum) containing compounds at 2X of the final
302 concentration indicated in the figures or figure legends (or 200 ng/ml PTX, List Biological Laboratories #179A)
303 were added to the top chamber of the wells and incubated for 1 hour at room temperature. After this
304 incubation period, 250 µl of medium supplemented with 400 ng/ml SDF-1 α was added to the bottom chamber
305 to create the chemotactic gradient. The concentration of compound and PTX in the bottom chamber was
306 matched to that in the top chamber, and the concentration of DMSO was maintained constant at 0.5% (v:v)
307 across all conditions. Medium without SDF-1 α in the bottom chamber was used a negative control for
308 migration. Plates were incubated at 37 °C in 5% CO₂ for 24 hr before quantifying cell migration as described
309 above.

310

311 **Cell viability assay**

312 Cells were seeded in 96-well culture plates as follows (number of cells per well in parenthesis): MDA-
313 MB-231 (7,500); MCF-7 (12,500); MCF-10A (7,500); Hs-578T (7,500); BT-549 (7,500); HeLa (7,500). Each
314 well contained 100 μ l of the complete medium for each cell line described in “*Cell culture and establishment*
315 *of cell lines*”. After an overnight growth period, the medium was aspirated and replaced with 100 μ l of the
316 appropriate medium containing the final concentration of compounds indicated in the figures or figure legends
317 or vehicle control (DMSO). DMSO concentration was equalized for all conditions in each experiment to 0.5%
318 (v:v). After 24 hours of incubation with compound, the medium was aspirated and replaced with 100 μ l of
319 CellTiterGlo (Promega, cat# G7570) diluted with medium (1:5 ratio) that had been equilibrated to room
320 temperature. The mixture was shaken for 2 minutes and incubated for 10 minutes at room temperature before
321 reading total luminescence in a Biotek Synergy H1 plate reader. Luminescent counts detected in wells
322 containing only medium were subtracted from all conditions, and the resulting counts were normalized to
323 counts in the DMSO-only control (100%) as a measure of cell abundance. In compound dose dependence
324 experiments, values of 3 technical replicates (wells) were averaged in each independent experiment.

325

326 Nuclear Magnetic Resonance (NMR)

327 All NMR data were measured on Bruker AVANCE 800 spectrometers equipped with cryogenically cooled
328 triple resonance z-gradient probes. Proton chemical shifts were referenced to internal 2,2-dimethyl-2-
329 silapentane-5-sulfonate (DSS, 0.00 ppm), and ^{13}C and ^{15}N chemical shifts were indirectly referenced to DSS
330 (31). The NMR Spectra were processed with TopSpin (Bruker) and analyzed with Sparky (32). Gai3 spectra
331 were recorded at 30 °C on 400 μ l samples in 5 mm Shigemi NMR tubes (without plunger) containing ^2H - ^{13}C -
332 ^{15}N –Gai3 in 10 mM HEPES pH 7.0 with 10 mM MgCl_2 , 5 mM DTT, 0.01 % NaN_3 and 5% $^2\text{H}_2\text{O}$ with either
333 300 μM GDP or 300 μM $\text{GTP}\gamma\text{S}$. The protein samples were prepared from a frozen stock solution of Gai3 in
334 10 mM HEPES pH 7.0, 150 mM NaCl, 1 mM DTT and 20 μM GDP) by three cycles of 4-fold dilution (into 10
335 mM HEPES pH 7.0, 10 mM MgCl_2 , 5 mM DTT, and 300 μM GDP or 300 μM $\text{GTP}\gamma\text{S}$) and concentration by
336 ultrafiltration using 10 kDa cut-off membranes. The NMR samples were prepared by addition of small volumes
337 of concentrated stocks of NaN_3 , $^2\text{H}_2\text{O}$ and DSS. The assignment of the NMR signals in the ^1H - ^{15}N TROSY of
338 Gai3-GDP was done based on the Biological Magnetic Resonance Data Bank (BMRB) entry 19015 (33)
339 corrected by adding 0.09 and -1.10 ppm to the ^1H and ^{15}N chemical shifts, respectively (2). The assignment
340 of the NMR signals in the ^1H - ^{15}N TROSY of Gai3- $\text{GTP}\gamma\text{S}$ was done based on the BMRB entry 18103 (33)
341 corrected by adding -0.05 and 0.58 ppm to the ^1H and ^{15}N chemical shifts, respectively (in this case, the
342 BMRB chemical shifts were measured at pH 6.5, which may explain in part the difference). Titrations were
343 done by the step wise addition of small volumes of a 10 mM solution of IGGi-11 in 50% aqueous DMSO
344 (Gai3-GDP) or a 100 mM solution of IGGi-11 in pure DMSO (Gai3- $\text{GTP}\gamma\text{S}$). The accumulated amount of
345 DMSO added to the protein sample at the last titration point was less than 2 %, too low to significantly affect
346 the chemical shift of the protein amide protons (34). The assignment of the NMR signals in the ^1H - ^{15}N TROSY

347 of Gai3 bound to IGG1-11 was based on the nearest neighbor approach along the titrations. The Chemical
348 Shift Perturbations were computed as the weighted average distance between the backbone amide ^1H and
349 ^{15}N chemical shifts in the free and bound states, as described (35). For those residues with no assigned
350 signal in the spectrum of free protein or without a reliable assignment in the bound protein, no chemical shift
351 perturbation could be calculated and classified as “no data” in the corresponding figure. For some residues
352 with weak signals in the spectrum of free Gai3, the intensity decreased in the bound form below three times
353 the level of the noise, beyond recognition as reliable signals, and are labeled as such in the corresponding
354 figure.

355

356 **Dose-dependence fluorescence polarization (FP) assay**

357 Unless otherwise indicated in the figures or figure legends, this assay was carried out with rat His-Gai3.
358 The composition of the assay buffer was 10mM HEPES, 10mM MgCl_2 , 0.0004% (v:v) NP-40, 5mM DTT, and
359 300 μM GDP, pH 7 with the exception of experiments shown in **Fig. S6**, which were done in buffer 50 mM
360 Tris, 100 mM NaCl, 10 mM MgCl_2 , 5 mM EDTA, 0.04% (v:v) NP-40, 30 μM GDP, 1 mM DTT, pH 7.4. In Figure
361 S6, the conditions with peptide KB-1753 also contained 30 μM AlCl_3 and 10 mM NaF (to generate the AlF_4^-
362 species that permits the association of Gai3 with this peptide (3)). Five μl of G α protein were added to black
363 384-well plates (OptiPlate-384F, Perkin Elmer cat#6007270), mixed with 10 μl of compound, and incubated
364 for 10 minutes at room temperature. Then, 5 μl of FITC-labeled peptide (GIV, R12 GL, KB-1753) were added
365 to each well, and incubated again for 10 min at room temperature protected from light before reading
366 fluorescence. Fluorescence polarization (Ex 485 ± 10 nm/Em 528 ± 10 nm) was measured every 2 min for
367 30 min at room temperature in a Biotek H1 synergy plate reader to ensure that the signals were stable in
368 time. Fluorescence polarization at different times was averaged for all subsequent calculations. The final
369 concentration of G α protein was 1 μM and the final concentration of peptides was 25 nM. Compounds were
370 at the concentrations indicated in the figures or figure legends, and the concentration of DMSO was equalize
371 to 1% (v:v) across all conditions, including negative controls without compound. Conditions containing FITC-
372 labeled peptides but no G-protein were included to determine the basal FP levels to be subtracted from all
373 conditions, which were subsequently normalized using the DMSO-only controls as 100% reference. Results
374 were fitted to a one-site competitive binding model inhibition curve to calculate the IC_{50} values using Prism
375 (GraphPad). IC_{50} values were converted to inhibitor constants (K_i) (36) by using previously determined
376 equilibrium dissociation constants (K_D) (2, 3).

377

378 **Computational docking of IGGi-11 on Gai3**

379 IGGi-11 was docked on a previously described (2) model of GIV-bound Gai3 (coordinates deposited at
380 www.modelarchive.org; 10.5452/ma-ayq5v). After removing GIV from the model, the structure of IGGi-11 was
381 docked using ICM version 3.8–3 (Molsoft LLC., San Diego, CA) by focusing on a region in the vicinity of Gai3

382 residues K35, K197, G217, S252, W258, and R313. IGGi-11 was treated as a fully flexible ligand in a rigid
383 receptor simulation within continuous dielectric solvent using internal coordinate mechanics (37, 38). Force
384 fields and energy potentials are determined with the modified Merck Molecular Force Field 94 (MMFF94) (39)
385 and the Empirical Conformation Energy Program for Peptides (ECEPP/3) (40) for small molecules and
386 proteins, respectively. Internal force field energy, receptor-ligand hydrogen bonding, hydrophobic energy,
387 conformational entropy loss, and solvation energy change were used for scoring and ranking of docking
388 poses. The maximum van der Waals repulsion was set to 4.0. The receptor maps had a grid size of 0.5
389 angstroms. No explicit waters were included in the simulation. Structure images were rendered with ICM
390 (Molsoft) or PyMol (Schrodinger).

391

392 **GST pull-down assay**

393 Assessment of protein-protein binding using GST pull-down assays was carried out as described
394 previously (4, 23, 41) with minor modifications. Briefly, 3 μg of GST-GIV (aa 1671-1755), GST-RGS4, or
395 GST were immobilized on glutathione agarose beads (ThermoFisher#16100) for 90 min at room temperature
396 in PBS. Beads were washed twice with PBS and resuspended in 250 μl of binding buffer (50 mM Tris-HCl,
397 pH 7.4, 100 mM NaCl, 0.04% (v:v) NP-40, 10 mM MgCl_2 , 5 mM EDTA, 1 mM DTT, 30 μM GDP), and
398 supplemented with test compounds (100 μM) or an equivalent volume of DMSO. After addition of 50 ng of (~
399 5 nM) of rat His-Gai3 purified, tubes were incubated for 4 hr at 4 $^{\circ}\text{C}$ with constant rotation. After this incubation,
400 beads were washed four times with 1 ml of wash buffer (4.3 mM Na_2HPO_4 , 1.4 mM KH_2PO_4 , pH 7.4, 137 mM
401 NaCl, 2.7 mM KCl, 0.1% (v/v) Tween-20, 10 mM MgCl_2 , 5 mM EDTA, 1 mM DTT, 30 μM GDP). For the
402 experiments testing binding of G proteins to RGS4, all buffers were supplemented with 30 μM AlCl_3 and 10
403 mM NaF to load Gai with $\text{GDP}\cdot\text{AlF}_4^-$. Resin-bound proteins were eluted by boiling for 5 min in Laemmli
404 sample buffer, and proteins were separated by SDS-PAGE and immunoblotted with antibodies as indicated
405 under "*Cell signaling stimulation, cell lysis, and immunoblotting*".

406

407 **Isothermal titration calorimetry (ITC)**

408 These experiments were carried out at 25 $^{\circ}\text{C}$ using a MicroCal iT200 system (Malvern Panalytical,
409 Malvern, UK). IGGi-11 was diluted from a 100 mM stock in DMSO to a final concentration of 1 mM in assay
410 buffer (10 mM HEPES, 10 mM MgCl_2 , 1 mM TCEP, 300 μM GDP, pH 7.0). Experiments were performed by
411 injecting 2 μl of this compound solution into a 200 μl solution containing 50 μM human His-Gai3 (WT or
412 mutants) supplemented with 1% DMSO in the sample cell. A total of 19 sequential injections were performed
413 with a spacing of 150 s and a reference power of 9 $\mu\text{cal/s}$. For each measurement session, a control
414 experiment to estimate heat of dilution was carried by compound titration into buffer without protein. The heat
415 of dilution was subtracted from each compound-protein titration, and the binding isotherms were plotted and

416 analyzed using Origin Software (MicroCal Inc., USA). Data were fit to a one-site binding model (N = 1). Each
417 protein was analyzed at least twice with similar results.

418

419 **Bioluminescence Resonance Energy Transfer (BRET) measurements in isolated membranes**

420 HEK293T cells were seeded on 6-well plates (~400,000 cells/well) coated with 0.1% gelatin and
421 transfected 24 hr later using the calcium phosphate method. For experiments using the free Gβγ biosensor
422 system, all conditions received the following amounts of plasmid per dish: 1.2 μg for VC-Gβ₁, 1.2 μg for VN-
423 Gy₂, and 0.3 μg mas-GRRK3ct-Nluc. In addition, plasmids for the following combinations of Gα subunit and
424 GPCR were co-transfected: 6 μg for Gai3 and 1.2 μg for α_{2A}-AR; 6 μg for Gαo and 1.2 μg for α_{2A}-AR; 6 μg
425 for Gαq-HA and 1.2 μg for M3R; and 6 μg for Gα13 and 1.2 μg for PAR1. For experiments aimed at detecting
426 Gai-GTP, cells were transfected with the following amounts of plasmid DNA per dish: 1.2 μg for α_{2A}-AR, 0.3
427 μg for mas-KB1753-Nluc, 3 μg for Gai3-YFP (b/c loop). Approximately 18-24 hr after transfection, cells were
428 scraped in PBS and pelleted at 550 x g for 5 min. Pellets from one 10-cm dish were resuspended in 250 μl
429 of ice-cold homogenization buffer (10 mM HEPES, 250 mM sucrose, 10 mM KCl, 1.5 mM MgCl₂, 1 mM DTT,
430 pH 7.4) supplemented with a protease inhibitor cocktail (Sigma, cat#8820). All subsequent steps were carried
431 out in ice or at 4 °C. Cells were homogenized by 30 passages through a 30-gauge needle and subsequently
432 centrifuged at 1,000xg for 10 min. The pellet was discarded and the supernatant transferred to a new tube
433 (Thermo Scientific, cat#314352) and centrifuged in a TLA-55 fixed angle rotor in a Beckman Coulter Optima
434 MAX-E tabletop centrifuge for 45 min at 100,000xg. The supernatant was aspirated, and the pellet was
435 resuspended in 250 μl of homogenization buffer by pipetting and syringing. This fraction containing isolated
436 cell membranes was stored as single-use 10 μl aliquots at -80 °C. Both endpoint and kinetic BRET
437 measurements were carried out in a final volume of 100 μl in 96-well plates. Briefly, 5 μl of isolated cell
438 membrane fraction was mixed with 85 μl of assay buffer (140 mM NaCl, 5 mM KCl, 1 mM MgCl₂, 1 mM CaCl₂,
439 0.37 mM NaH₂PO₄, 24 mM NaHCO₃, 10 mM HEPES, 0.1% (w:v) glucose, 1mM DTT, 0.002% (w:v) BSA, pH
440 7.4, supplemented with protease inhibitor cocktail at one-tenth of the recommended concentration for cell
441 lysates) containing the required amounts of IGGi-11 to achieve the final concentration of compound indicated
442 in the figure or figure legends. The concentration of DMSO was equalized to 1% (v:v) across all conditions.
443 In the experiments to assess the association of Gβγ with Gα in the absence of GPCR stimulation, the buffer
444 was supplemented with 300 μM GDP (Alfa Aesar #J61646), except for the control condition containing
445 GTPγS, in which GDP was replaced by 300 μM GTPγS (Sigma G8634). As an additional control condition in
446 these experiments, the buffer was supplemented with 25 μM of the R12 GL peptide, a Gai binding peptide
447 previously reported to disrupt its association with Gβγ (42). In the experiments to assess the dissociation of
448 Gβγ from Gα or for the formation of Gai3-GTP upon GPCR stimulation, the buffer was supplemented with
449 300 μM GTP (MB Bioscience #151216), except for the control conditions containing GTPγS, in which GTP
450 was replaced by 300 μM GTPγS (Sigma G8634). GPCR agonists were used as follows: 1 μM brimonidine

451 (Ark Pharm, cat# AK-3579) for experiments with Gi, 0.1 μM brimonidine for experiments with Go, 100 μM
452 carbachol (Acros Organics cat# AC-10824) for experiments with Gq, and 30 μM Thrombin Receptor Activator
453 Peptide 6 (TRAP-6, Anaspec cat# AS-24190) for experiments with G13. For all endpoint experiments,
454 membrane/compound mixtures were incubated for 3 min at room temperature before adding 10 μl of
455 coelenterazine 400a to obtain a final concentration of 5 μM . Two minutes after the addition of coelenterazine
456 400a, luminescence signals were measured in a POLARstar OMEGA plate reader (BMG Labtech) at 28 °C.
457 Luminescence was measured at 450 ± 40 and 535 ± 15 nm, and BRET was calculated as the ratio between
458 the emission intensity at 535 ± 15 nm divided by the emission intensity at 450 ± 40 nm. Ratios determined
459 from three consecutive measurements spaced by 36 s were averaged. Results were presented as the BRET
460 change relative to an untreated condition (no IGGi-11 and not GPCR agonist). The procedures were similar
461 for kinetic BRET measurements, except that luminescence signals were measured every 0.24 s for the
462 duration of the experiment, and that brimonidine (0.1 μM) and yohimbine (100 μM) were injected into the
463 wells during the measurements as indicated in the figures. Results for the kinetic BRET measurements were
464 presented as the BRET change relative to the baseline signal (the average BRET ratio in the 30 s before
465 agonist stimulation).

466

467 **Adenylyl cyclase activity in isolated membranes**

468 Two million HEK293T cells were seeded on gelatin coated 10 cm dishes. Eighteen hours later, cells were
469 transfected with 6 μg of a plasmid DNA encoding human AC5-YFP using the calcium phosphate method.
470 Twenty-four hours after transfection, cells were scraped in PBS and pelleted by centrifugation at $550\times g$ for 5
471 minutes. Cell pellets were re-suspended in homogenization buffer and membranes isolated as described in
472 "*Bioluminescence Resonance Energy Transfer (BRET) measurements in isolated membranes*". Membrane
473 pellets were resuspended in 250 μl of homogenization buffer, and protein content quantified by Bradford.
474 Aliquots were stored at -80 °C until their use in experiments. Adenylyl cyclase activity in membranes was
475 determined by the production of cAMP under different conditions. Reactants were mixed on ice in a final
476 volume of 40 μl of assay buffer (50 mM HEPES, 2 mM MgCl_2 , 1 mM EDTA, 0.5 mg/mL BSA, pH 8.0) as
477 follows. All conditions were done in duplicate. Four μl of IGGi-11 or vehicle (DMSO) were mixed with 8 μl of
478 myr-G α i1-GTP γ S (or the same volume of buffer for conditions without G α i1) and incubated for 10 minutes
479 before the addition of 2 μg of AC5-expressing membrane protein in a volume of 8 μl . Next, 8 μl of G α s-GTP γ S,
480 forskolin or buffer were added and tubes were incubated on ice for 10 minutes. Reactions were started by
481 adding pre-warmed ATP and MgCl_2 solution in a volume of 4 μl and rapidly transferring the tubes to a heat
482 block at 30 °C for 10 minutes. Reactions were stopped by heating tubes at 95°C for 5 minutes, then
483 centrifuged and an aliquot from the supernatant was taken to quantify cAMP using the LANCE cAMP kit
484 (Perkin Elmer, cat#AD0262) according to the manufacturer protocol. The final concentrations of reactants
485 were: IGGi-11, 100 μM ; DMSO, 0.1 % (v:v); myr-G α i1-GTP γ S, 1 μM , G α s-GTP γ S, 0.1 μM ; forskolin (Tocris,

486 cat#1099), 10 μ M; ATP, 1 mM; $MgCl_2$, 5 mM. myr-Gai1 and G α s were loaded with GTP γ S by incubating
487 them at 30 °C with 150 μ M GTP γ S in buffer (20 mM Tris-HCl, 20 mM NaCl, 1 mM $MgCl_2$, 1 mM DTT, 5 %
488 glycerol (v:v) for 3 hours or 45 minutes, respectively. Time-resolved fluorescence measurements to quantify
489 cAMP were done on a TECAN Infinite M1000 plate reader in white 384-well ProxiPlates (Perkin Elmer,
490 cat#6008280). Specific activity was expressed as pmol cAMP / min / mg membrane after background
491 subtraction of the cAMP signal obtained in the absence of membranes. Values of 2 duplicates were averaged
492 in each independent experiment.

493

494 **Steady-state GTPase assay**

495 This assay was performed as described previously (4, 6, 23, 41) with minor modifications. Briefly, purified
496 human His-Gai3 WT (500 nM) or human His-Gai1 R178M/A326S (Gai1^{RM/AS}, 50 nM) was pre-incubated for
497 15 min at 30 °C in assay buffer (20 mM Na-HEPES, 100 mM NaCl, 1 mM EDTA, 2 mM $MgCl_2$, 1 mM DTT,
498 and 0.05% (w:v) C₁₂E₁₀, pH 8) with the concentrations of IGGi-11, His-GIV-CT, R12 GL peptide, or His-RGS4
499 indicated in the figures or figure legends. GTPase reactions were initiated at 30 °C by adding an equal volume
500 of assay buffer containing 1 μ M [γ -³²P]GTP (~50 c.p.m./fmol). Duplicate aliquots (25 μ L) were removed at 10
501 min and reactions stopped with 975 μ l of ice-cold 5% (w:v) activated charcoal in 20 mM H₃PO₄, pH 3. Samples
502 were then centrifuged for 10 min at 10,000xg, and 500 μ l of the resultant supernatant were scintillation-
503 counted to quantify the amount of [³²P]Pi released. Background [³²P]Pi detected at 10 min in the absence of
504 G protein was subtracted from each reaction. Background counts were <5% of the counts detected in the
505 presence of G proteins. Results were calculated as relative to the activity of the G-protein alone (% of control).

506

507 **GTP γ S-BODIPY binding assay**

508 GTP γ S-BODIPY (Life Technologies, cat#G22183) was diluted in 100 μ l of assay buffer (20 mM Na-
509 HEPES, 100 mM NaCl, 1 mM EDTA, 2 mM $MgCl_2$, 1 mM DTT, 0.05% (w:v) C₁₂E₁₀, pH 8) to a final
510 concentration of 50 nM in the presence of 30 μ M IGGi-11, 30 μ M NF023 (a positive control for inhibition of
511 GTP binding to Gai proteins (43)), or an equivalent amount of DMSO (0.1% v:v). After approximately 15 min
512 incubation at 28 °C, fluorescence measurements were carried out at the same temperature by exciting at
513 485 nm and detecting emission at 535 \pm 30 nm in a POLARstar OMEGA plate reader (BMG Labtech) every
514 30 seconds. Purified human His-Gai3 (200 nM) was added in real time during the measurements as indicated
515 in the figures.

516

517 **Membrane permeability and hydrolytic processing of compounds**

518 Membrane permeability of IGGi-11 or IGGi-11me was assessed using a parallel artificial membrane
519 permeability assay (PAMPA) kit (BioAssay Systems, cat#PAMPA-096) following the manufacturer's
520 instructions with minor modifications. Briefly, an artificial membrane was reconstituted over a porous support

521 that separated the donor (upper) from an acceptor (bottom) well with a 4% (w:v) lecithin solution in dodecane.
522 100 µl of a solution containing compound diluted in PBS buffer (pH 7.4) at a final concentration of 20 µM in
523 5% (v:v) DMSO were added to the upper well, and 220 µl of 5% (v:v) DMSO in PBS buffer were added to the
524 bottom well. After incubation for 6 hours at 37 °C, 90 µl or 200 µl were taken from the upper or bottom well,
525 respectively, and transferred to microcentrifuge tubes (Olympus 1.7ml Microtube Cat# 24-282LR) that were
526 stored at -80 °C. All conditions were done in duplicate. Samples were dried in a speed vacuum centrifuge
527 and reconstituted with 0.1% (v:v) formic acid in water (90 µl or 30 µl for sample from the upper or the bottom
528 wells, respectively) by vortexing. Samples were analyzed by LC-MS/MS. Chromatography was performed
529 using a Waters Acquity CSH™ Phenyl-Hexyl 1.7µM 2.1 x 50mm column and acetonitrile/water as the mobile
530 phase, and a Sciex API 4000 triple quadrupole mass spectrometer with an ESI source was used in positive
531 mode with a full MS scan at 55.0-1000 m/z. Compound abundance was estimated from the area under the
532 spectral curve (AUC) in FreeStyle 1.8 SP1 software (ThermoFisher). For the experiments assessing the
533 hydrolytic processing of IGGi-11me into IGGi-11, samples were analyzed the same way by LC-MS/MS with
534 some modifications in the procedure for sample preparation. Briefly, 90 µl of 20 µM IGGi-11me diluted in
535 PBS with 5% (v:v) DMSO was incubated in the presence or absence of 25 µg of a cytosolic fraction of MDA-
536 MB-231 cells (44) for 2 hours at 37 °C or not incubated at all (time 0). All conditions were done in duplicate.
537 Samples were extracted by mixing with 8 volume parts of an organic solution (8:1:1
538 Acetonitrile:Methanol:Acetone), incubation at 4 °C for 30 minutes, and centrifugation at 15,000xg for 15 min
539 at 4 °C. The extracted clear supernatant was transferred to a clean tube and dried in a speed vacuum
540 centrifuge. Samples were reconstituted with 90 µl of 0.1% (v:v) formic acid in water by vortexing before
541 injection into the LC-MS/MS instrument.

542

543 **Cell signaling stimulation, cell lysis, and immunoblotting**

544 Two-hundred thousand MDA-MB-231 cells or 250,000 HeLa cells per well were seeded on 6-well plates.
545 Twenty-four hours after seeding, cells were incubated overnight (~16 h) before EGF (Recombinant Human
546 Epidermal Growth Factor, GoldBiotechnnology, cat#1150-04-100) stimulation with the concentrations of IGGi-
547 11me indicated in the figures or figure legends or a matching amount of DMSO (0.25% v:v) in the presence
548 of 0.5% (v:v) or 0.2% (v:v) FBS for MDA-MB-231 or HeLa cells, respectively. For experiments using SDF-
549 1α (R&D Systems, 350-NS/CF) instead of EGF for stimulation, cells were incubated overnight before
550 stimulation in the absence of FBS. In some cases, cells were also pre-incubated overnight with pertussis
551 toxin (PTX, 100 ng/ml, List Biological Laboratories #179A). Cells were stimulated with EGF or SDF-1α as
552 indicated in the figures or figure legends by adding concentrated stocks to the wells. Stimulation reactions
553 were stopped by rapidly washing with ice-cold PBS three times and adding 100 µl of lysis buffer (20 mM
554 HEPES, 5 mM Mg(CH₃COO)₂, 125 mM K(CH₃COO), 0.4% (v:v) Triton X-100, 1 mM DTT, 10 mM β-
555 glycerophosphate, and 0.5 mM Na₃VO₄, pH 7.4) supplemented with a protease inhibitor cocktail (Sigma, cat#

556 S8830) per well before harvesting by scraping. Whole cell lysates were cleared by centrifugation (10 min at
557 $14,000 \times g$, 4°C , and then quantified by Bradford (Bio-Rad, cat#5000205), and boiled in Laemmli sample
558 buffer for 5 min before protein separation by SDS-PAGE and electrophoretic transfer to PVDF membranes
559 (EMD Millipore, cat#IPFL00010) for 2 hr. PVDF membranes were blocked with TBS supplemented with 5%
560 non-fat dry milk for 1 hr, and then incubated sequentially with primary and secondary antibodies. Primary
561 antibody species, vendors, and dilutions were as follows: GIV (Rabbit, Santa Cruz Biotechnology, sc-133371);
562 total Akt (Mouse, Cell Signaling Technologies, 2920), 1:2000; phosphorylated Akt (S473) (Rabbit, Cell
563 Signaling Technologies, 9271), 1:1000; Gai3 (Rabbit, Aviva, #OAAB19207), 1:250; Gai1/2 (Rabbit, Sigma,
564 06-236) 1:250; β -actin (mouse, LiCor Biosciences, 926-42212), 1:2500; GST (Rabbit, Sigma, G7781), 1:2500;
565 His (mouse, Sigma, H1029), 1:2500. Secondary antibodies (goat anti-rabbit conjugated to AlexaFluor 680
566 (Life Technologies, #A-21077) or goat anti-mouse conjugated to IRDye 800 (LI-COR Biosciences, #926–
567 32210) were used at 1:10,000. Infrared imaging of immunoblots was performed according to manufacturer's
568 recommendations using an Odyssey CLx infrared imaging system (LI-COR Biosciences). Akt activation was
569 determined by calculating the phospho-Akt (pAkt)/ total-Akt ratio and normalizing it to the maximum activation
570 in each experiment (percentage of maximal response). Images were processed using the ImageJ software
571 (NIH) and assembled for presentation using Photoshop and Illustrator software (Adobe). The same protocol
572 of cell lysis and immunoblotting was followed to detect the expression of proteins in any other cell line under
573 steady state culture condition or for the detection of proteins in GST pulldown experiments.

574

575 **Bioluminescence Resonance Energy Transfer (BRET) measurements in HeLa cells**

576 BRET experiments with already generated HeLa cells stably expressing biosensor constructs for Gai-
577 GTP (Gai*-BERKY3) or for free $G\beta\gamma$ ($G\beta\gamma$ -BERKY3) were carried out as described previously (30).

578

579 **Luminescence-based cAMP measurements in cells**

580 Approximately 300,000 HEK293T cells were seeded on each well of 6-well plates coated with 0.1% (w/v)
581 gelatin, and transfected ~24 hr later using the calcium phosphate method with plasmids encoding the
582 following constructs as indicated in the figures (DNA amounts in parentheses): $GABA_B R1a$ (0.2 μg),
583 $GABA_B R2$ (0.2 μg), α_{2A} -AR (0.2 μg), and Glosensor 22F (0.8 μg). Total DNA amount per well was equalized
584 to 2 μg by supplementing with pcDNA3.1. Cell medium was changed 6 h after transfection, and cells were
585 treated overnight with 100 μM IGGi-11me or vehicle (DMSO) as indicated in the figures.

586 For kinetic measurements, approximately 16-24 h after transfection, cells were washed and gently
587 scraped in room temperature PBS, centrifuged (5 min at $550 \times g$), and resuspended in 750 μl Tyrode's buffer
588 (140 mM NaCl, 5 mM KCl, 1 mM MgCl_2 , 1 mM CaCl_2 , 0.37 mM NaH_2PO_4 , 24 mM NaHCO_3 , 10 mM HEPES
589 and 0.1% glucose, pH 7.4). Two-hundred μl of cells were mixed with 200 μl of 5 mM D-luciferin K^+ salt

590 (GoldBio, LUCK-100) diluted in buffer (140 mM NaCl, 5 mM KCl, 1 mM MgCl₂, 1 mM CaCl₂, 0.37 mM
591 NaH₂PO₄, 20 mM HEPES and 0.1% glucose, pH 7.4) and incubated at 28 °C for 15 minutes. Ninety µl of
592 cells pre-incubated with D-luciferin were added to a white opaque 96-well plate (Opti-Plate, PerkinElmer Life
593 Sciences, 6005290) before measuring fluorescence. Fluorescence signal was measured without filters at
594 28 °C every 10 s in a BMG Labtech POLARStar Omega plate reader. Kinetic traces are represented as raw
595 fluorescence signal. Percentage (%) inhibition was calculated at ~360 s post-isoproterenol stimulation using
596 the response to isoproterenol without pretreatment as the 100% reference. All conditions were baseline
597 subtracted before calculations.

598 For dose response experiments, approximately 16-24 h after transfection, cells were washed and
599 gently scraped in room temperature PBS, centrifuged (5 min at 550 × g), and resuspended in 300 µl Tyrode's
600 buffer. Two-hundred and forty µl of cells were mixed with 240 µl of 5 mM D-luciferin K⁺ salt diluted in buffer
601 (140 mM NaCl, 5 mM KCl, 1 mM MgCl₂, 1 mM CaCl₂, 0.37 mM NaH₂PO₄, 20 mM HEPES and 0.1% glucose,
602 pH 7.4) and incubated at 28 °C for 15 minutes. Twenty µl of different concentrations of brimonidine or GABA
603 diluted in Tyrode's buffer as 4X the final concentration in the assay were added to wells of a white opaque
604 96-well plate. 37.6 µl of additional Tyrode's buffer was added to wells. 22.4 µl of cells pre-incubated with D-
605 luciferin were added to wells using an electronic multichannel pipette and incubated for 2 minutes at room
606 temperature. Immediately after, 20 µl of a 5X stock of isoproterenol (to achieve a final concentration of 100
607 nM in the assay) diluted in Tyrode's buffer were added to wells using an electronic multichannel pipette and
608 measurement was started. Luminescence signal was measured without filters at 28 °C every 30 s in a BMG
609 Labtech POLARStar Omega plate reader. Brimonidine or GABA mediated inhibition of isoproterenol induced
610 cAMP responses were calculated at ~300 s and are represented relative to the response to isoproterenol
611 alone.

612

613 **Matrigel cultures**

614 MDA-MB-231 or MCF10A cells were cultured on top of Matrigel as described previously (29, 45) with
615 minor modifications. Briefly, 25 µl of ice-cod Matrigel (growth factor reduced, Corning, #356231) were spread
616 as a thick layer on the bottom of 96-well plates (Thermo 167008) and allowed to solidify at 37 °C. Two-
617 thousand and five hundred cells were seeded on the Matrigel-coated wells in a volume of 100 µl of their
618 regular growth medium supplemented with 2% (v:v) Matrigel. Six hours after cell seeding, the medium was
619 replaced with 100 µl of the same medium supplemented with 100 µM IGGi-11me or vehicle (0.5% DMSO).
620 All conditions were done in duplicates. Medium was replaced every other day by fresh medium without
621 compound. Cell abundance was estimated on days 0, 2, 4, 5, and 7 using CellTiter-Glo® (Promega, G7570)
622 as described in "Cell viability assays" section. Relative Luminescence Unit (RLU) values of the technical
623 replicates (wells) were averaged in each independent experiment. For imaging of Matrigel cultures, cells
624 were grown under equivalent conditions but in 8-well glass bottom chambers (Cellvis, cat# C8-1.5H-N). Briefly,

625 5,000 cells were seeded on wells coated with 40 μ l of Matrigel in a volume of 200 μ l. Images were acquired
626 7 days after seeding by phase-contrast microscopy with a Zeiss Axio Observer Z1 microscope equipped with
627 a camera (C10600/Orca-R2; Hamamatsu Photonics) using 10x (NA= 0.45; working distance 2 mm) or 20x
628 (NA= 0.8; working distance 0.55 mm) objectives. Images were acquired and processed using Zeiss' ZEN
629 software and assembled for presentation using Photoshop and Illustrator software (Adobe).

630

631 **Mouse xenografts**

632 Half a million MDA-MB-231 cells stably expressing fluc2-myc were seeded on 10 cm dishes. Twenty-
633 four hours after seeding, medium was replaced with DMEM supplemented with 0.2% FBS and 100 μ M IGGi-
634 11me or vehicle (0.5% DMSO) and dishes placed in the cell incubator overnight. After this, cells were
635 detached by incubation with warm citric saline solution (135 mM KCl, 15 mM sodium citrate, pH 7.2), washed
636 three times with serum-free DMEM, and resuspended in serum-free DMEM at a concentration of 2×10^7
637 cells/ml. One-hundred μ l of this suspension of cells were subcutaneously injected in the hind flank of ~8
638 week-old female NCr nu/nu athymic nude mice (Taconic Bioscience, cat#NCRNU-F). Tumor cells were
639 visualized using whole-body bioluminescence imaging (BLI) using an IVIS® Spectrum In Vivo Imaging
640 System (Perkin Elmer) 3-5 minutes after intraperitoneal injection of 150 mg/kg D-luciferin potassium salt
641 (GoldBiotechnology, cat#LUCK-1G) dissolved in PBS (Corning, 21-040-CV) and filtered through a 0.45- μ m
642 surfactant-free cellulose acetate (SFCA) membrane filter. Photon count per second per square centimeter
643 per steradian (p/sec/cm²/sr) values and images were acquired using Living Images software (Perkin Elmer).
644 At the end of experiments, flank injected tumors were removed and photographed. All individual images were
645 processed using Living Images software and assembled for presentation using Photoshop and Illustrator
646 software (Adobe). All animal procedures were approved by the IACUC of Boston University under protocol
647 PROTO201800258.

648 In parallel to the above, MDA-MB-231 cells treated with IGGi-11me and resuspended in citric saline as
649 described for the xenograft injection experiments were assessed for growth on plastic dishes under standard
650 culture conditions. Briefly, MDA-MB-231 cells from the citric saline suspension were reconstituted in DMEM
651 supplemented with 10% FBS and seeded on wells of a 96-well plate in a volume of 100 μ l (1,000 cells/ well).
652 All conditions were done in triplicates. Cell abundance was estimated on days 0, 1, 2, and 3 using CellTiter-
653 Glo® (Promega, G7570) as described in "Cell viability assays" section, and Relative Luminescence Unit (RLU)
654 values of the technical replicates (wells) were averaged in each independent experiment. Results were
655 expresses as Relative cell growth using the counts in day 0 to normalize.

656

657

658

659
660
661
662
663
664
665
666
667
668
669
670
671
672
673
674
675
676
677
678
679
680
681
682
683
684
685
686

FIGURE S1

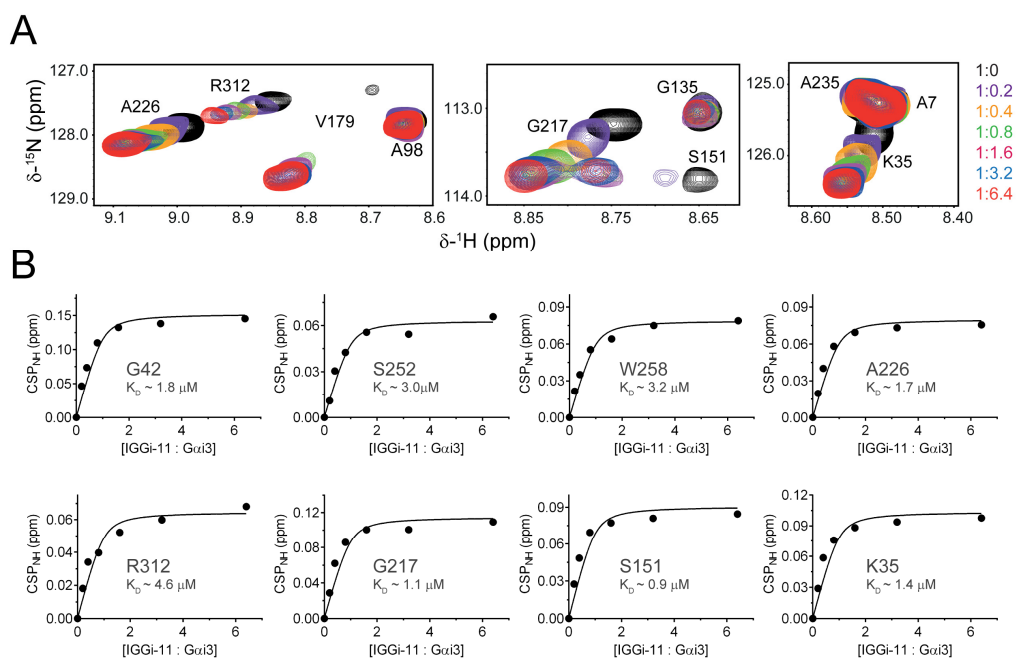


Figure S1. Gai3 NMR signal perturbations upon IGGi-11 titration. (A) Overlay of ^1H - ^{15}N -TROSY spectra of ^2H , ^{13}C , ^{15}N -Gai3-GDP after addition of increasing amounts of IGGi-11. Colors correspond to the molar Gai3:IGGi-11 ratios indicated on the right. **(B)** Plots of the measured chemical shift perturbation (CSP) values of selected Gai3 residues fitted to a single-site binding model to estimate equilibrium dissociation constants.

687
688
689
690
691
692
693
694
695
696
697
698
699
700
701
702
703
704
705
706
707
708
709
710
711
712
713
714
715
716
717
718
719
720
721

FIGURE S2

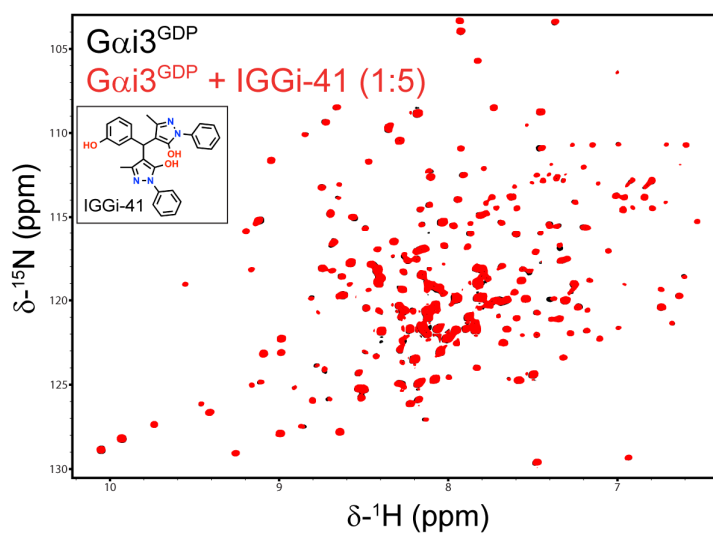
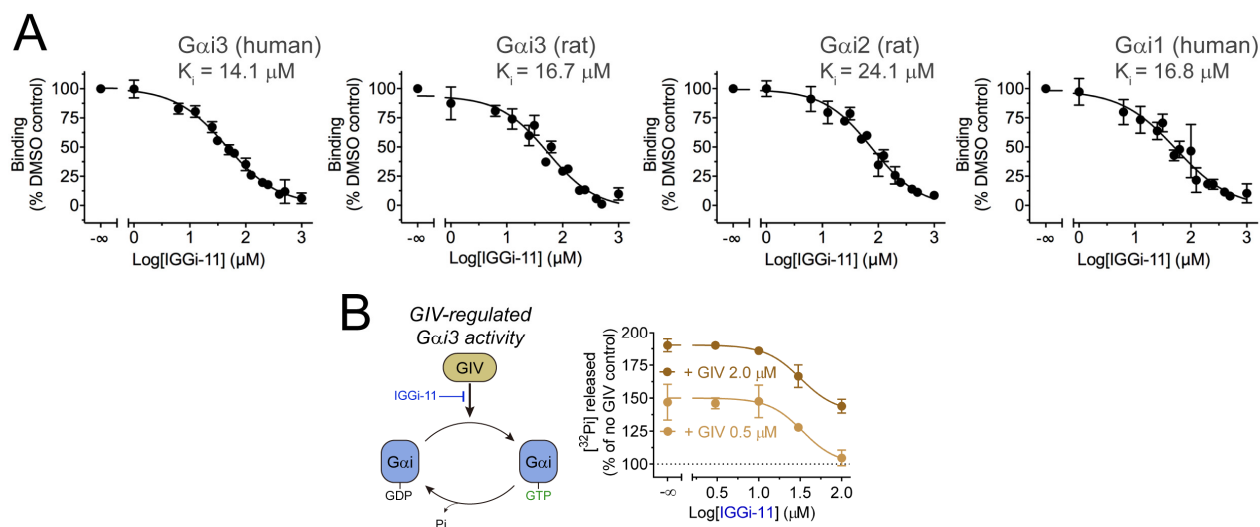


Figure S2. IGGi-41 does not induce NMR signal perturbations on Gai3. (A) Overlay of $^1\text{H}\text{-}^{15}\text{N}$ TROSY spectra of $^2\text{H}, ^{13}\text{C}, ^{15}\text{N}$ -Gai3-GDP in the absence or presence of IGGi-41 in five-fold molar excess, showing minimal perturbations caused by the compound.

722
723
724
725
726
727
728
729

FIGURE S3



730
731
732
733
734
735
736
737
738
739
740
741
742
743
744

Figure S3. IGGi-11 inhibits binding of GIV to different Gai subunits, and blocks GIV-mediated G protein activity regulation *in vitro*. (A) Quantification of GIV binding to different Gai proteins by fluorescence polarization in the presence of increasing concentrations of IGGi-11. K_i values were determined from the curve fits as indicated in *Methods*. Results are expressed as mean \pm SEM ($N = 3$). (B) IGGi-11 inhibits GIV-mediated stimulation of Gai3 steady-state GTPase activity. The steady-state GTPase activity of Gai3, which depends on the rate of nucleotide exchange, was determined in the presence of 0.5 or 2 μ M GIV-CT and increasing concentrations (1–100 μ M) of IGGi-11 by measuring the production of [32 P]P_i from GTP[γ - 32 P]. Results are expressed as % of the activity of Gai3 in the absence of GIV. Mean \pm S.E.M ($N = 3$).

FIGURE S4

745
746
747
748
749
750
751
752
753
754
755
756
757
758
759
760
761
762
763
764
765
766
767
768
769
770
771
772
773
774
775
776
777
778
779

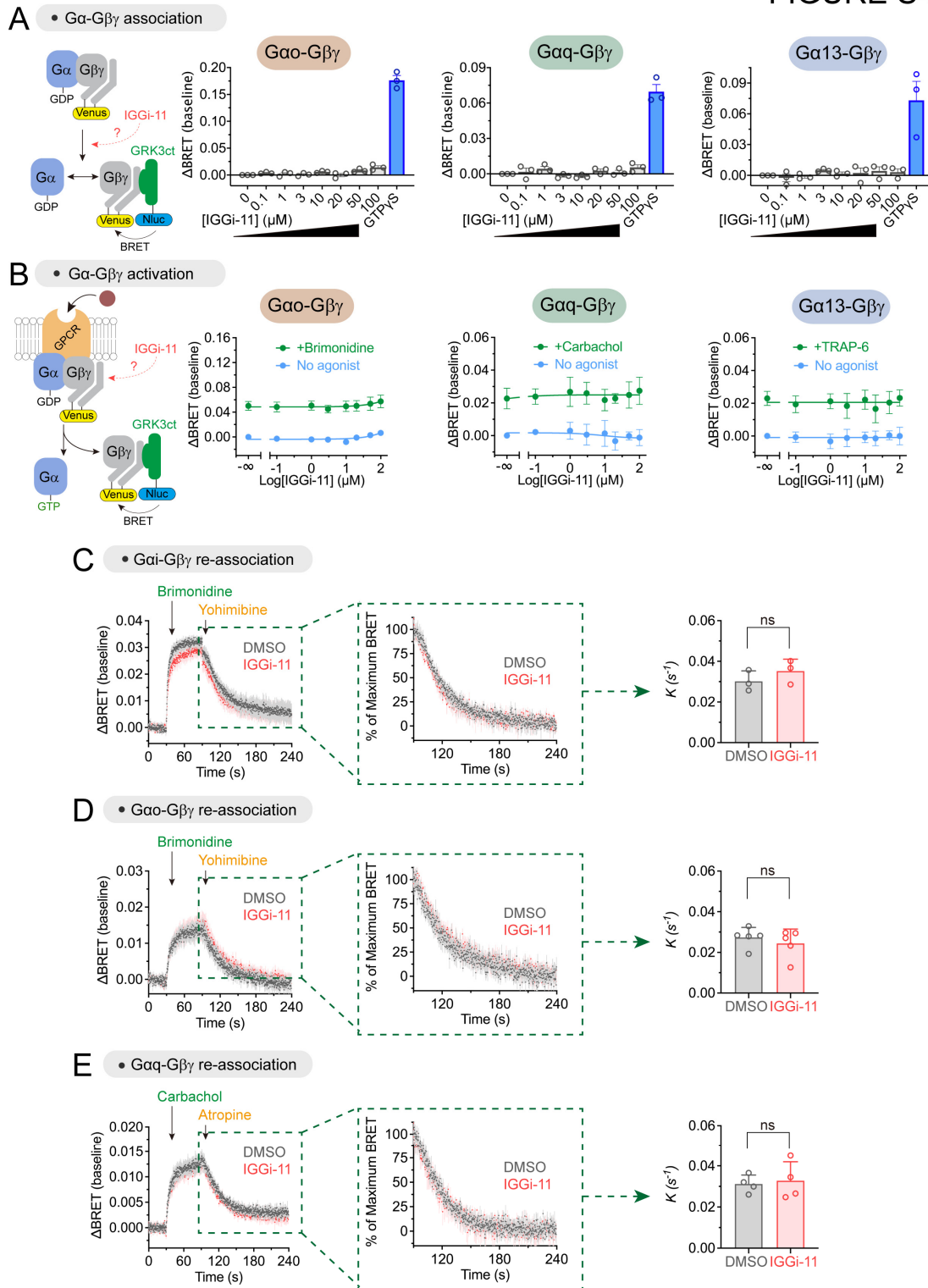


Figure S4. Lack of effect of IGGi-11 on G-protein heterotrimer association, re-association, or coupling to GPCRs. (A) IGGi-11 does not dissociate Gβγ from Gao, Gaq or Gα13 in membranes isolated from HEK293T cells expressing a BRET-based biosensor for free Gβγ, whereas GTPγS (300 μM) does. (B) IGGi-11 does not affect GPCR-mediated activation of Go, Gq or G13 in membranes isolated from HEK293T cells as determined by the dissociation of Gα-Gβγ heterotrimers using BRET-based biosensors. The α_{2A}

780 adrenergic receptor, the M3 muscarinic receptor, or the PAR1 receptor were co-expressed for experiments
781 with Go, Gq or G13, respectively. Membranes were treated with the indicated concentrations of IGGi-11 with
782 (green) or without (blue) stimulation with a receptor agonist (1 μ M brimonidine for Go, 100 μ M carbachol for
783 Gq, and 30 μ M Thrombin Receptor Activator Peptide 6 (TRAP-6) for G13) for 2 minutes before BRET
784 measurements. **(C, D, E)** IGGi-11 does not interfere with G $\beta\gamma$ re-association with Gai3 (C), Gao (D), or Gaq
785 (E) upon termination of GPCR stimulation. Membranes isolated from HEK293T cells co-expressing Gai3,
786 Gao, or Gaq with a cognate GPCR (α_{2A} adrenergic receptor for Gi and Go, M3R for Gq), and the components
787 of a BRET-based biosensor for free G $\beta\gamma$ were treated with an agonist and antagonist indicated during
788 continuous kinetic luminescence measurements as indicated in the figure. Concentrations were as follows:
789 0.1 μ M brimonidine , 100 μ M yohimbine, 100 μ M carbachol, and 100 μ M atropine. Deactivation rates (k) were
790 determined by fitting normalized deactivation data after antagonist addition to an exponential decay curve.
791 All data are mean \pm SEM ($N = 3-5$). ns = $P > 0.05$, ANOVA.

792

793

794

795

796

797

798

799

800

801

802

803

804

805

806

807

808

809

810

811

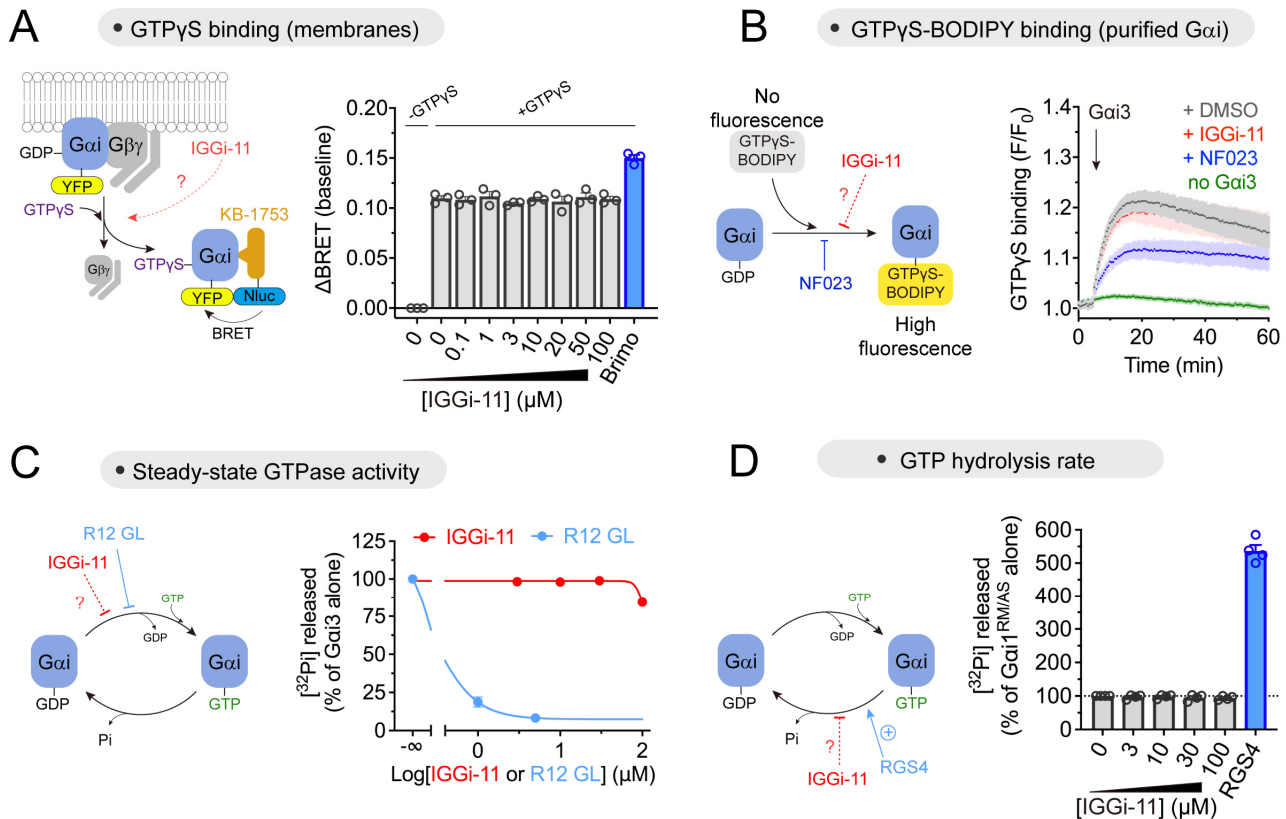
812

813

814

815
816
817
818
819

FIGURE S5



820

821 **Figure S5. Lack of effect of IGGi-11 on nucleotide handling by G-proteins.** (A) IGGi-11 does not affect
 822 spontaneous GTPγS binding to Gai3 as determined by BRET-based detection of Gai3-GTP in isolated cell
 823 membranes. Membranes isolated from HEK293T cells expressing a BRET-based biosensor for Gai3-GTP
 824 were incubated with GTPγS (300 μM) and the indicated concentrations of IGGi-11. GPCR stimulation with
 825 brimonidine (1 μM) increases GTPγS binding. Mean ± SEM (N = 3). (B) IGGi-11 does not affect spontaneous
 826 GTPγS binding to purified Gai3 as determined by a fluorescent analog assay. Purified Gai3 was added to a
 827 solution containing GTPγS-BODIPY and the increase in fluorescence caused by binding of the nucleotide to
 828 the G-protein monitored continuously in the presence of 30 μM IGGi-11 or NF023 (a positive control for
 829 inhibition of nucleotide binding by Gai (43)), or DMSO (1 %) as the negative control. Mean ± SEM of 3
 830 independent experiments. (C) IGGi-11 does not affect Gai3 steady-state GTPase activity. The steady-state
 831 GTPase activity of Gai3, which depends on the rate of nucleotide exchange, was determined in the presence
 832 of increasing concentrations (3-100 μM) of IGGi-11 or the GoLoco peptide R12 GL (1-5 μM, positive inhibition

833 control), by measuring the production of [³²P]P_i from GTP[γ-³²P]. Results are expressed as % of the activity
834 of Gai3 alone. Mean ± S.E.M (N = 3). **(D)** IGGi-11 does not affect GTP hydrolysis by Gai. The steady-state
835 GTPase activity of the Gai1^{RM/AS} mutant, which depends on the rate of nucleotide hydrolysis but not of
836 nucleotide exchange (46), was determined in the presence of increasing concentrations (3-100 μM) of IGGi-
837 11 or 0.8 μM of the GAP RGS4 (positive control for enhancement of nucleotide hydrolysis), by measuring the
838 production of [³²P]P_i from GTP[γ-³²P]. Results are expressed as % of the activity of Gai1^{RM/AS} alone. Mean ±
839 S.E.M (N = 4).

840

841

842

843

844

845

846

847

848

849

850

851

852

853

854

855

856

857

858

859

860

861

862

863

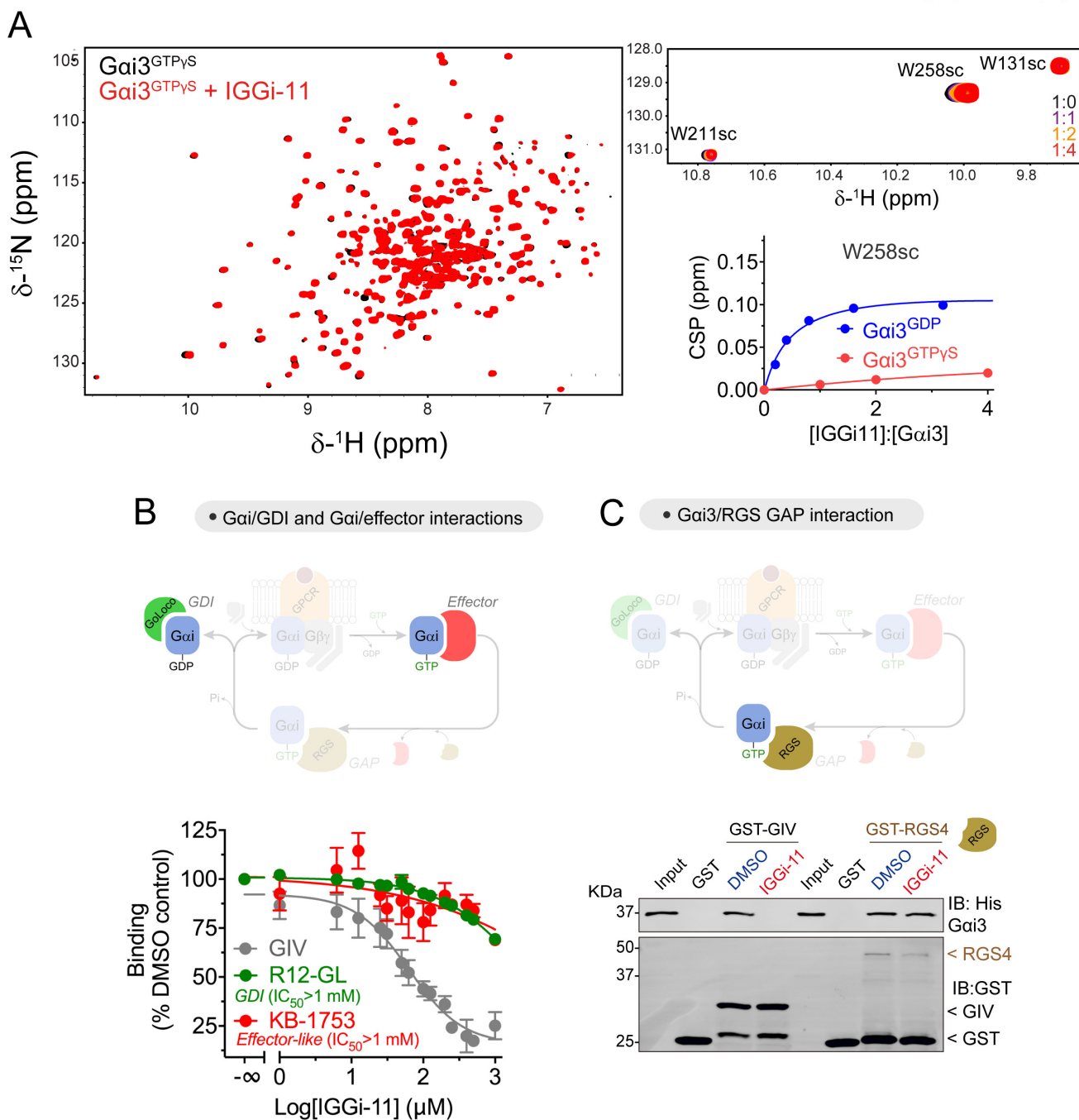
864

865

866

867

FIGURE S6



868

869 **Figure S6. IGGi-11 does not bind to GTP-bound Gai3 or prevent Gai3 binding to GDIs, GAPs or**
 870 **effectors. (A)** Overlay of ^1H - ^{15}N TROSY spectra of ^2H , ^{13}C , ^{15}N -Gai3-GTP γ S in the absence or presence of
 871 IGGi-11 display minimal perturbations by the compound. A selected region containing signals for the side
 872 chains of W211 and W258, which undergo large perturbation in GDP-bound Gai3 in the presence of IGGi-11
 873 (**Fig. 2**), is shown enlarged on the upper right. The lower right plot compares the chemical shift perturbation
 874 (CSP) values of the side chain of W258 in GDP- or GTP γ S-bound Gai3 upon IGGi-11 titration. (**B**) IGGi-11
 875 inhibits GIV binding but does not inhibit the binding of a GoLoco GDI peptide or an effector-like peptide to rat

876 Gai3, while it blocks GIV binding. Binding of a GIV peptide, a GDI peptide corresponding to the GoLoco motif
877 of RGS12 (R12-GL), or the effector-like peptide KB-1753 to Gai3 was quantified by fluorescence polarization.
878 GIV and R12-GL experiments were done in the presence of GDP, whereas KB-1753 experiments were done
879 in the presence of GDP+AlF₄⁻. Mean ± SEM (N = 3). **(C)** IGGi-11 disrupts GIV-Gai3 binding but not GAP-
880 Gai3 binding in pulldown assays. Gai3 was incubated with glutathione agarose-bound GST-GIV (aa 1671-
881 1755) or GST-RGS4 in the presence of IGGi-11 (100 μM) or DMSO (1%). After incubation and washes, bead-
882 bound proteins were separated by SDS-PAGE and immunoblotted (IB) as indicated. Conditions with GIV
883 contained GDP, whereas those with RGS4 contained GDP + AlF₄⁻ to induce the formation of the transition
884 state recognized by GAPs. One experiment representative of 3 independent repeats is presented.

885

886

887

888

889

890

891

892

893

894

895

896

897

898

899

900

901

902

903

904

905

906

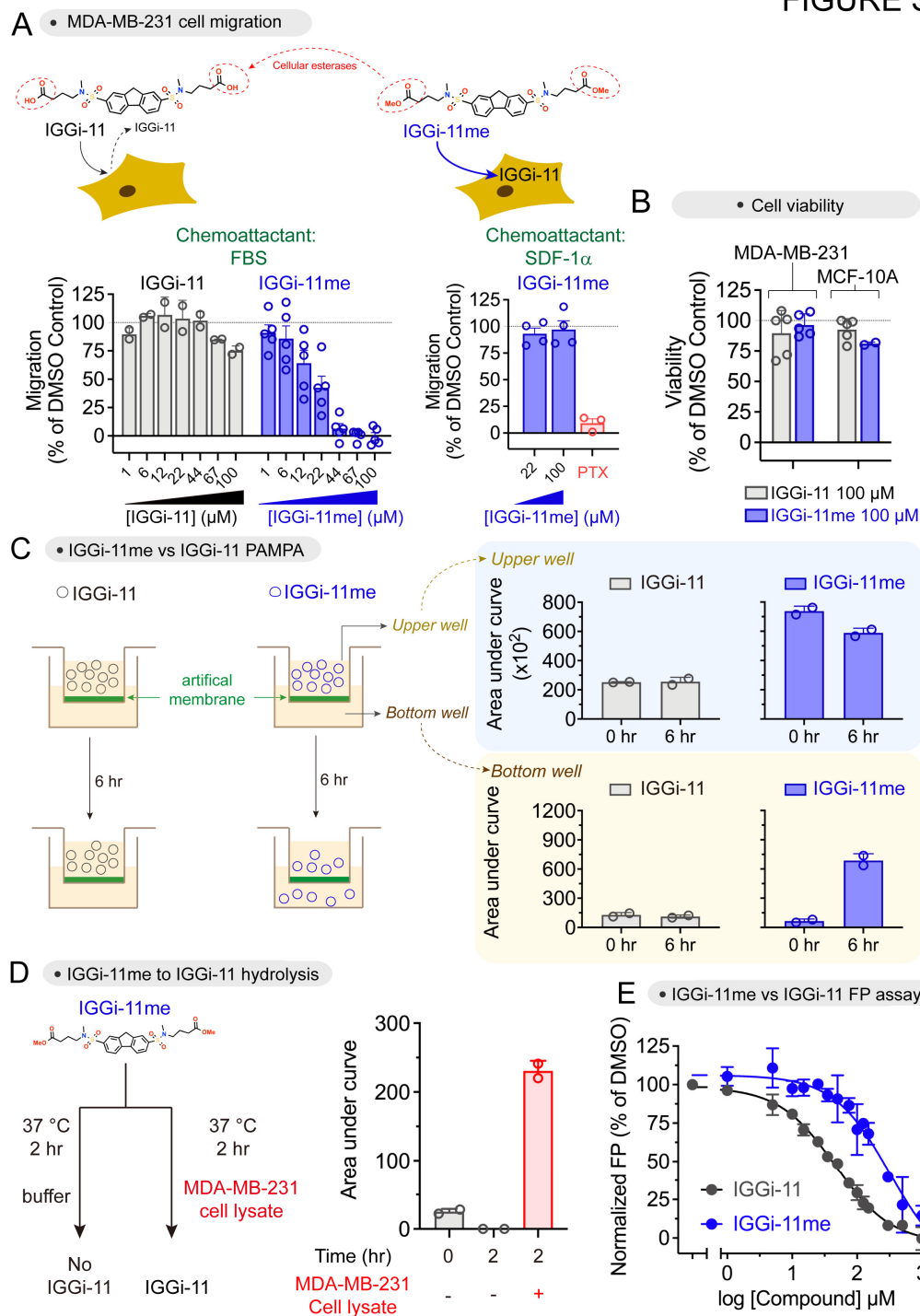
907

908

909

910

FIGURE S7



911
912
913
914
915
916
917
918
919
920
921
922
923
924
925
926
927
928
929
930
931
932
933
934
935
936
937
938

Figure S7. IGGi-11me is a membrane permeable analog of IGGi-11 that is bioactive in cells. (A) Top, diagram depicting a putative mechanism by which IGGi-11me acts in cells. Esterification of IGGi-11's carboxylate groups to generate IGGi-11me is proposed to increase membrane permeability, whereas action of cellular esterases on IGGi-11me leads to formation of the active compound IGGi-11. IGGi-11me, but not IGGi-11, efficiently blocks MDA-MB-231 cell migration stimulated by FBS as the chemoattractant (bottom left) but does not block migration stimulated by the CXCR4 agonist SDF-1 α (bottom right). Cell migration was determined using a modified Boyden-chamber assay in the presence of the indicated concentrations of

946 compound (1-100 μ M). Pertussis toxin (PTX, 100 ng/ml), which uncouples Gi from GPCRs like CXCR4 was
947 used as positive control. Results are expressed as % of migration compared to cells treated with DMSO (1 %).
948 Mean \pm S.E.M ($N = 2-5$) **(B)** Neither IGGi-11 nor IGGi-11me affect the viability of MDA-MB-231 or MCF-10A
949 cells. Results are expressed as % of viability of cells treated with 100 μ M compound compared to cells treated
950 with DMSO (1 %). Mean \pm S.E.M ($N = 2-5$). **(C)** IGGi-11me displays higher permeability than IGGi-11 in
951 parallel artificial membrane permeability assays (PAMPA). The presence of IGGi-11 or IGGi-11me in the
952 upper and lower wells of the PAMPA assays was determined by LC-MS before and 6 hours after addition of
953 compound to the upper well. Duplicates of one experiment representative of two are presented. **(D)** IGGi-
954 11me is converted to IGGi-11 by cellular esterases. IGGi-11me was incubated in the presence or absence of
955 a cytosolic fraction of MDA-MB-231 cells for 2 hours and the amount of IGGi-11 present in the sample was
956 determined by LC-MS. Duplicates of one experiment representative of two are presented. **(E)** IGGi-11me
957 is less potent than IGGi-11 as an inhibitor of the GIV-G α i interaction. Binding of GIV to rat G α i3 was
958 determined by fluorescence polarization in the presence of different concentrations of the indicated
959 compounds. Mean \pm S.E.M ($N = 3$).

960

961

962

963

964

965

966

967

968

969

970

971

972

973

974

975

976

977

978

979

980

FIGURE S8

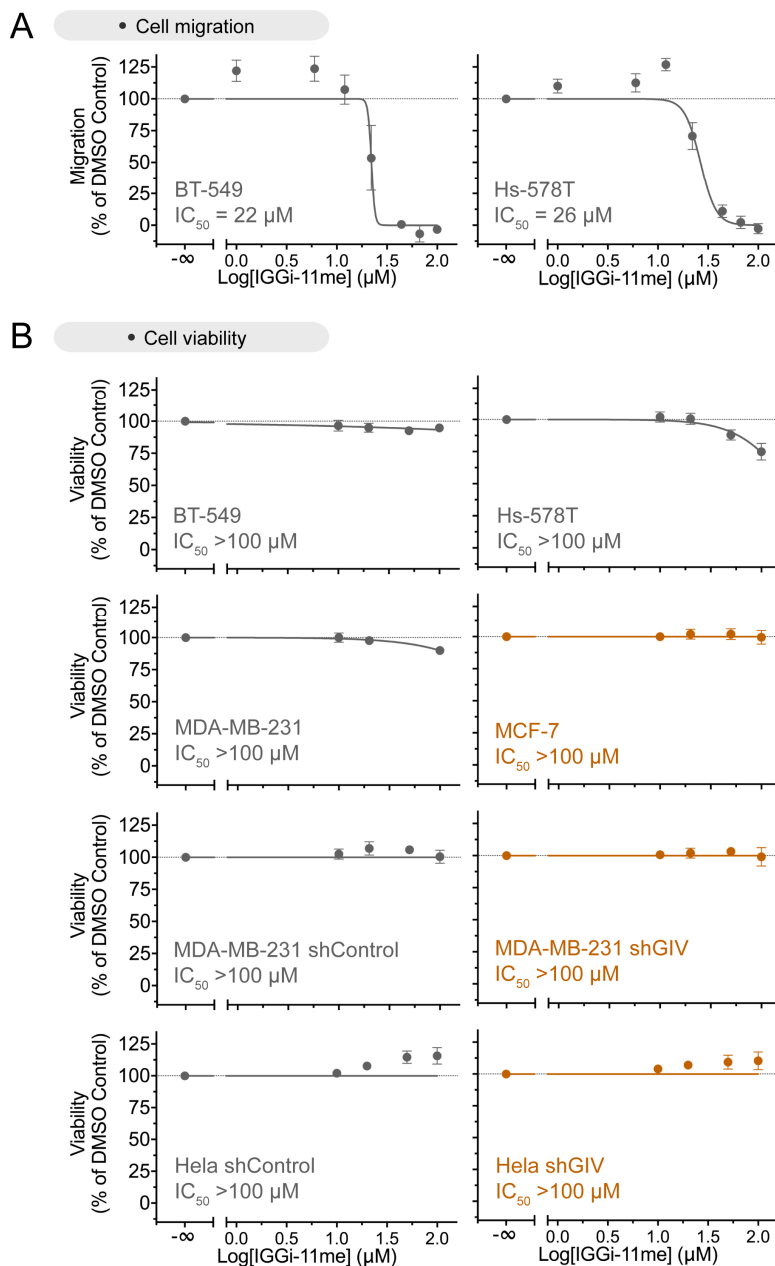
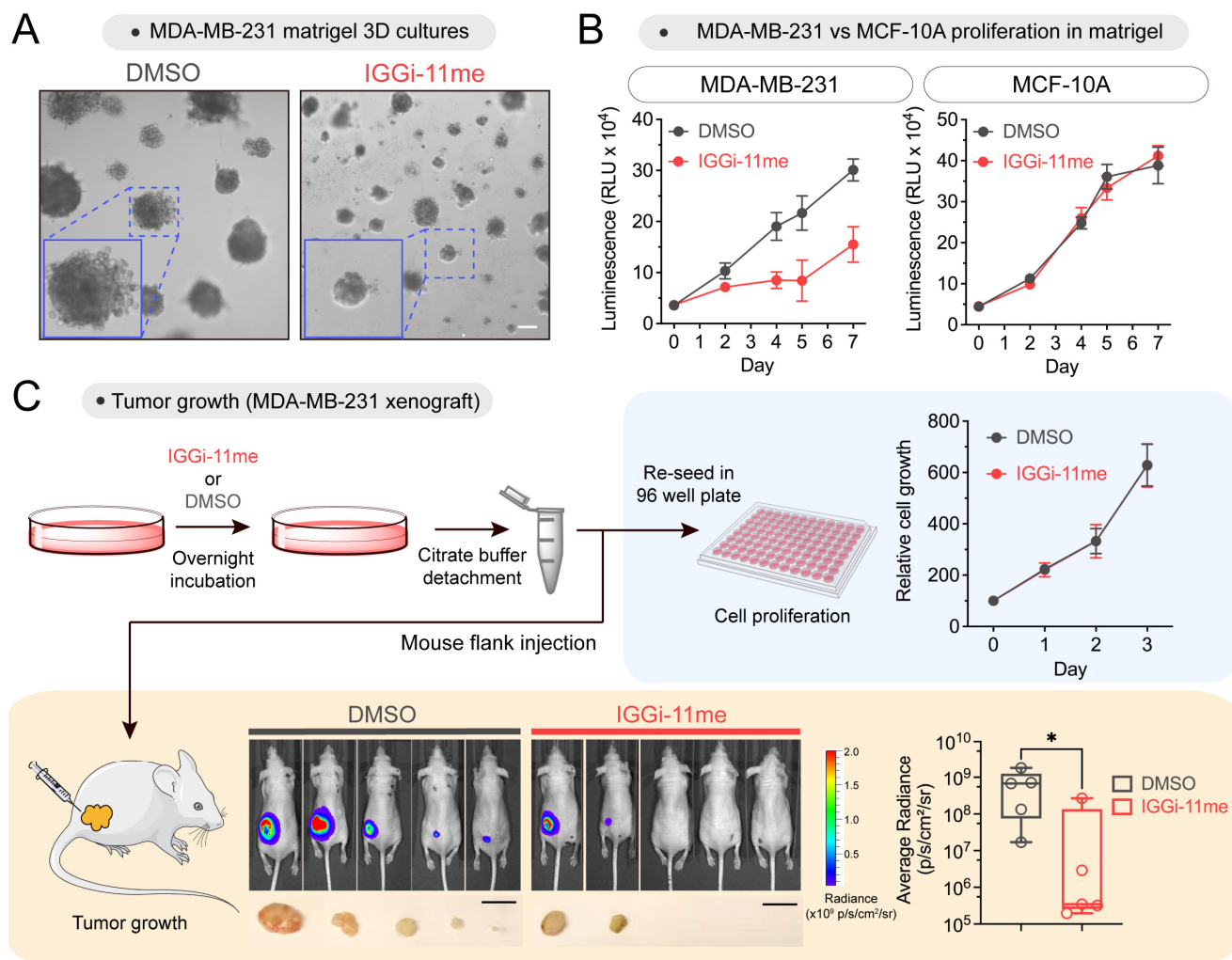


Figure S8. IGGi-11me blocks cell migration in GIV^{High} cells, but does not affect cell viability in multiple cell lines. (A) IGGi-11me blocks migration of BT-549 and Hs578T cells, two GIV^{High} cell lines (Fig. 5). Cell migration was determined using a modified Boyden-chamber assay in the presence of the indicated concentrations of compound (1-100 μM). Results are expressed as % of migration compared to cells treated with DMSO (1 %). Mean ± S.E.M (N = 3) (B) IGGi-11me does not affect the viability of GIV^{High} cells (BT-549, Hs578T, MDA-MB-231, or HeLa cell lines), GIV^{Low} (MCF-7), or GIV-depleted MDA-MB-231 or HeLa cells. Results are expressed as % of viability of cells treated with the indicated concentrations of compound (1-100 μM) compared to cells treated with DMSO (1 %). Mean ± S.E.M (N = 3).

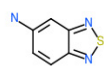
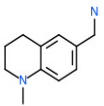
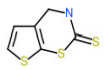
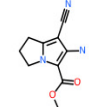
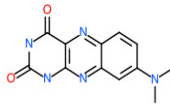
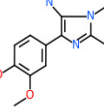
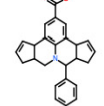
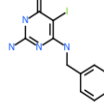
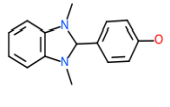
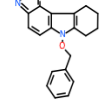
FIGURE S9



017

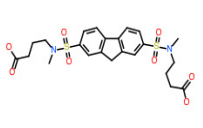
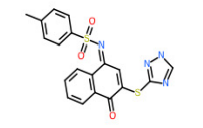
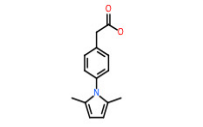
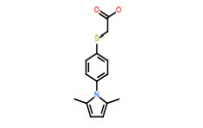
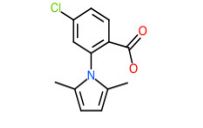
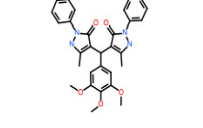
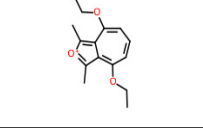
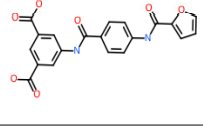
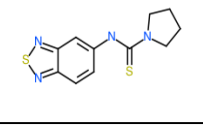
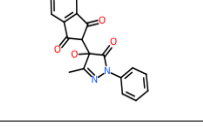
018 **Figure S9. IGGi-11me inhibits cancer cell growth in tumor-like contexts.** (A, B) IGGi-11me inhibits
 019 growth of MDA-MB-231 breast cancer invasive cells, but not of non-transformed MCF-10A cells, on Matrigel.
 020 IGGi-11me (100 μM) or DMSO was used to treat cells at the onset of the culture period for 2 days and then
 021 removed for the remaining duration of the experiment. (A) displays representative images of acini at 7 days
 022 (scale bar = 100 μm), and viability in (B) is expressed as mean ± SEM (N ≥ 3). (C) IGGi-11me impairs
 023 Pretreatment of MDA-MB-231 cells with IGGi-11me impairs growth when subsequently implanted in mice but
 024 not when seeded on culture dishes. MDA-MB-231 cells treated overnight with IGGi-11me (100 μM) or DMSO
 025 were resuspended in citrate saline buffer and either injected subcutaneously in female NCr nu/nu athymic
 026 nude mice or seeded on plastic culture dishes. Mice were imaged 8 weeks later upon luciferin administration
 027 (N = 5 per group) and tumors were photographed post-mortem (scale bar = 1 cm). Box plots on the left
 028 display the quantification of luminescence (median, min/max). *P < 0.05, Mann-Whitney U test. Cell growth
 029 on culture dishes was quantified as in (B).

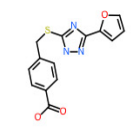
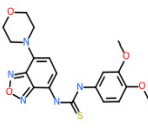
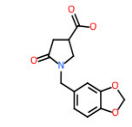
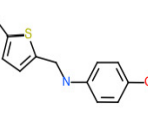
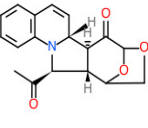
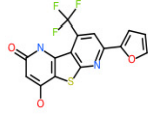
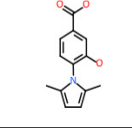
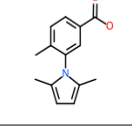
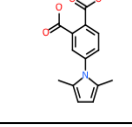
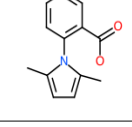
030 TABLE S1

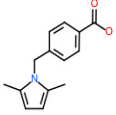
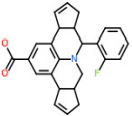
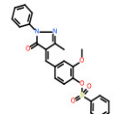
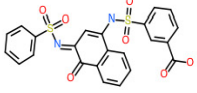
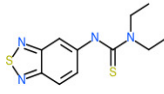

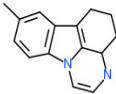
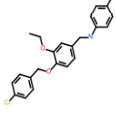
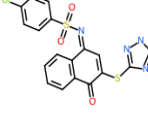
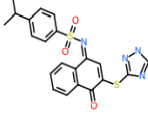
Structure	IGGi ID	Scaffold	molWeight	Source	IUPAC Name
	1	Singleton	151.0	ChemBridge	2,1,3-benzothiadiazol-5-amine
	2	G	176.1	ChemBridge	(1-methyl-3,4-dihydro-2H-quinolin-6-yl)methanamine
	3	Singleton	187.0	ChemBridge	3,4-dihydrothieno[3,2-e][1,3]thiazine-2-thione
	4	Singleton	205.1	ChemBridge	methyl 2-amino-1-cyano-6,7-dihydro-5H-pyrrolizine-3-carboxylate
	5	E	257.1	ChemBridge	8-(dimethylamino)-1H-benzo[g]pteridine-2,4-dione
	6	Singleton	255.1	ChemBridge	4-(3-aminoimidazo[1,2-a]pyridin-2-yl)-2-methoxyphenol
	7	G	369.2	ChemBridge	2-phenyl-1-azapentacyclo[10.6.1.03,7.08,19.013,17]nonadeca-5,8,10,12(19),14-pentaene-10-carboxylic acid
	8	F	342.0	ChemBridge	2-amino-4-(benzylamino)-5-iodo-1H-pyrimidin-6-one
	9	Singleton	240.1	ChemBridge	4-(1,3-dimethyl-2H-benzimidazol-2-yl)phenol
	10	Singleton	319.1	ChemBridge	6-phenylmethoxy-7,8,9,10-tetrahydro-[1,2,5]oxadiazolo[3,4-c]carbazole

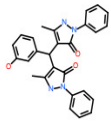
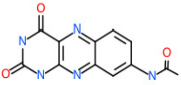
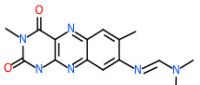
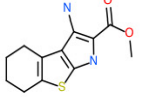
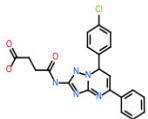
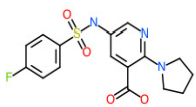
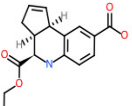
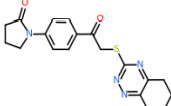
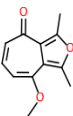
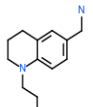
031

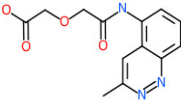
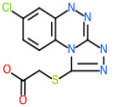
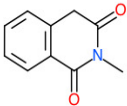
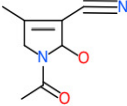
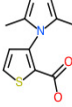
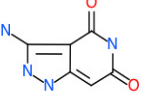
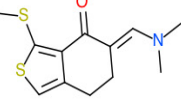
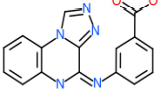
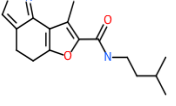
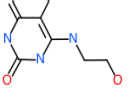
032

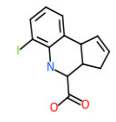
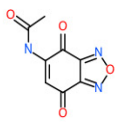
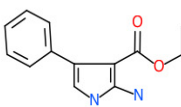
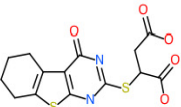
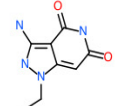
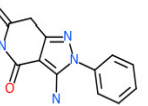
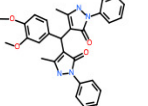
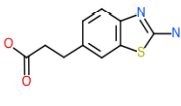
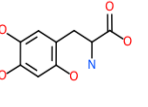
	11	C	524.1	ChemBridge	4'-((9H-fluorene-2,7-disulfonyl)bis(methylazanediyl))dibutyric acid
	12	B	410.1	ChemBridge	4-methyl-N-[4-oxo-3-(1H-1,2,4-triazol-5-yl)sulfanyl)naphthalen-1-ylidene]benzenesulfonamide
	13	I	229.1	ChemBridge	2-[4-(2,5-dimethylpyrrol-1-yl)phenyl]acetic acid
	14	I	261.1	ChemBridge	2-[4-(2,5-dimethylpyrrol-1-yl)phenyl]sulfanylacetic acid
	15	I	249.1	ChemBridge	4-chloro-2-(2,5-dimethylpyrrol-1-yl)benzoic acid
	16	A	526.2	ChemBridge	5-methyl-4-[(5-methyl-3-oxo-2-phenyl-1H-pyrazol-4-yl)-(3,4,5-trimethoxyphenyl)methyl]-2-phenyl-1H-pyrazol-3-one
	17	Fragment	247.1	ChemBridge	(4-ethoxy-1,3-dimethylcyclohepta[c]furan-8-ylidene)-ethyloxidanium
	18	J	394.1	ChemBridge	5-[[4-(furan-2-carbonylamino)benzoyl]amino]benzene-1,3-dicarboxylic acid
	19	D	264.1	ChemBridge	N-(2,1,3-benzothiadiazol-5-yl)pyrrolidine-1-carbothioamide
	20	A	334.1	ChemBridge	2-(4-hydroxy-3-methyl-5-oxo-1-phenylpyrazol-4-yl)indene-1,3-dione

	21	Singleton	301.1	ChemBridge	4-[[5-(furan-2-yl)-1H-1,2,4-triazol-3-yl]sulfanylmethyl]benzoic acid
	22	D	415.1	ChemBridge	1-(3,4-dimethoxyphenyl)-3-(4-morpholin-4-yl-2,1,3-benzoxadiazol-7-yl)thiourea
	23	Singleton	263.1	ChemBridge	1-(1,3-benzodioxol-5-ylmethyl)-5-oxopyrrolidine-3-carboxylic acid
	24	J	219.1	ChemBridge	4-[(5-methylthiophen-2-yl)methylamino]phenol
	25	Singleton	311.1	ChemBridge	(2S,3S,13R,14S)-3-acetyl-17,19-dioxo-4-azapentacyclo[14.2.1.02,14.04,13.05,10]nonadeca-5,7,9,11-tetraen-15-one
	26	C	352.0	ChemBridge	11-(furan-2-yl)-6-hydroxy-13-(trifluoromethyl)-8-thia-3,10-diazatricyclo[7.4.0.02,7]trideca-1(9),2(7),5,10,12-pentaen-4-one
	27	I	231.1	ChemDiv	4-(2,5-dimethylpyrrol-1-yl)-3-hydroxybenzoic acid
	28	I	229.1	ChemDiv	3-(2,5-dimethylpyrrol-1-yl)-4-methylbenzoic acid
	29	I	259.1	ChemDiv	4-(2,5-dimethylpyrrol-1-yl)phthalic acid
	30	I	215.1	ChemDiv	2-(2,5-dimethylpyrrol-1-yl)benzoic acid

	31	I	229.1	ChemDiv	4-[(2,5-dimethylpyrrol-1-yl)methyl]benzoic acid
	32	G	387.2	ChemDiv	2-(2-fluorophenyl)-1-azapentacyclo[10.6.1.03,7.08,19.013,17]nonadeca-5,8,10,12(19),14-pentaene-10-carboxylic acid
	33	A	448.1	ChemDiv	[2-methoxy-4-[(3-methyl-5-oxo-1-phenylpyrazol-4-ylidene)methyl]phenyl]benzenesulfonate
	34	B	496.0	ChemDiv	3-[[3-(benzenesulfonamido)-4-oxonaphthalen-1-ylidene]amino]sulfonylbenzoic acid
	35	D	266.1	ChemDiv	3-(2,1,3-benzothiadiazol-5-yl)-1,1-diethylthiourea
	36	B	325.1	ChemDiv	4-ethyl-N-(4-oxonaphthalen-1-ylidene)benzenesulfonamide
	37	Singleton	224.1	ChemDiv	12-methyl-1,4-diazatetracyclo[7.6.1.05,16.010,15]hexadeca-2,9(16),10(15),11,13-pentaene
	38	J	383.1	ChemDiv	4-[[4-[(4-chlorophenyl)methoxy]-3-ethoxyphenyl]methylamino]phenol
	39	B	430.0	ChemDiv	4-chloro-N-[4-oxo-3-(1H-1,2,4-triazol-5-ylsulfanyl)naphthalen-1-ylidene]benzenesulfonamide
	40	B	438.1	ChemDiv	N-[4-oxo-3-(1H-1,2,4-triazol-5-ylsulfanyl)naphthalen-1-ylidene]-4-propan-2-ylbenzenesulfonamide

	41	A	452.2	ChemDiv	4-[(3-hydroxyphenyl)-(5-methyl-3-oxo-2-phenyl-1H-pyrazol-4-yl)methyl]-5-methyl-2-phenyl-1H-pyrazol-3-one
	42	E	271.1	ChemDiv	N-(2,4-dioxo-1H-benzo[g]pteridin-8-yl)acetamide
	43	E	312.1	ChemDiv	N'-(3,7-dimethyl-2,4-dioxo-1H-benzo[g]pteridin-8-yl)-N,N-dimethylmethanimidamide
	44	C	250.1	ChemDiv	methyl 1-amino-5,6,7,8-tetrahydro-3H-[1]benzothio[2,3-b]pyrrole-2-carboxylate
	45	Singleton	423.1	ChemDiv	4-[[7-(4-chlorophenyl)-5-phenyl-4,7-dihydro-[1,2,4]triazolo[1,5-a]pyrimidin-2-yl]amino]-4-oxobutanoic acid
	46	B	365.1	ChemDiv	5-[(4-fluorophenyl)sulfonylamino]-2-pyrrolidin-1-ylpyridine-3-carboxylic acid
	47	H	287.1	ChemDiv	(3aS,4R,9bR)-4-ethoxycarbonyl-3a,4,5,9b-tetrahydro-3H-cyclopenta[c]quinoline-8-carboxylic acid
	48	Singleton	368.1	Asinex	1-[4-[2-(5,6,7,8-tetrahydro-1,2,4-benzotriazin-3-yl)sulfanyl)acetyl]phenyl]pyrrolidin-2-one
	49	Fragment	204.1	Asinex	4-methoxy-1,3-dimethylcyclohepta[c]furan-8-one
	50	G	204.2	Asinex	(1-propyl-3,4-dihydro-2H-quinolin-6-yl)methanamine

	51	Singleton	275.1	Maybridge	2-[2-[(3-methylcinnolin-5-yl)amino]-2-oxoethoxy]acetic acid
	52	Singleton	297.0	Maybridge	2-[(7-chloro-4,5-dihydro-[1,2,4]triazolo[3,4-c][1,2,4]benzotriazin-1-yl)sulfanyl]acetic acid
	53	Singleton	175.1	Maybridge	2-methyl-4H-isoquinoline-1,3-dione
	54	Singleton	166.1	Maybridge	1-acetyl-2-hydroxy-4-methyl-2,5-dihydropyrrole-3-carbonitrile
	55	I	221.1	Maybridge	3-(2,5-dimethylpyrrol-1-yl)thiophene-2-carboxylic acid
	56	Fragment	166.0	Maybridge	3-amino-4-hydroxy-1,5-dihydropyrazolo[4,3-c]pyridin-6-one
	57	Singleton	253.1	Maybridge	(5E)-5-(dimethylaminomethylidene)-3-methylsulfanyl-6,7-dihydro-2-benzothiophen-4-one
	58	Singleton	305.1	ChemDiv	3-([1,2,4]triazolo[4,3-a]quinoxalin-4-ylamino)benzoic acid
	59	C	287.2	ChemDiv	8-methyl-N-(3-methylbutyl)-4,5-dihydro-1H-furo[2,3-g]indazole-7-carboxamide
	60	F	297.0	TimTec	6-(2-hydroxyethylamino)-5-iodo-1H-pyrimidine-2,4-dione

	61	H	341.0	TimTec	6-iodo-3a,4,5,9b-tetrahydro-3H-cyclopenta[c]quinoline-4-carboxylic acid
	62	Singleton	207.0	Ambinter	N-(4,7-dioxo-2,1,3-benzoxadiazol-5-yl)acetamide
	63	Singleton	230.1	Ambinter	ethyl 2-amino-4-phenyl-1H-pyrrole-3-carboxylate
	64	C	354.0	Ambinter	2-[(4-oxo-5,6,7,8-tetrahydro-3H-[1]benzothio[2,3-d]pyrimidin-2-yl)sulfanyl]butanedioic acid
	65	Fragment	194.1	Ambinter	3-amino-1-ethyl-4-hydroxy-5H-pyrazolo[4,3-c]pyridin-6-one
	66	A	242.1	Ambinter	3-amino-2-phenyl-7H-pyrazolo[4,3-c]pyridine-4,6-dione
	67	A	496.2	Ambinter	4-[(3,4-dimethoxyphenyl)-(5-methyl-3-oxo-2-phenyl-1H-pyrazol-4-yl)methyl]-5-methyl-2-phenyl-1H-pyrazol-3-one
	68	Singleton	222.0	Sigma	3-(2-amino-1,3-benzothiazol-6-yl)propanoic acid
	69	Singleton	213.1	Sigma	2-amino-3-(2,4,5-trihydroxyphenyl)propanoic acid

040 **SUPPLEMENTARY REFERENCES**

- 041 1. Aznar N, *et al.* (2015) Daple is a novel non-receptor GEF required for trimeric G protein activation in
042 Wnt signaling. *Elife* 4:e07091.
- 043 2. de Opakua AI, *et al.* (2017) Molecular mechanism of Galphai activation by non-GPCR proteins with a
044 Galpha-Binding and Activating motif. *Nat Commun* 8:15163.
- 045 3. DiGiacomo V, de Opakua AI, Papakonstantinou MP, Nguyen LT, Merino N, Blanco-Canosa JB, Blanco
046 FJ, & Garcia-Marcos M (2017) The Galphai-GIV binding interface is a druggable protein-protein
047 interaction. *Sci Rep* 7(1):8575.
- 048 4. Garcia-Marcos M, Ghosh P, Ear J, & Farquhar MG (2010) A structural determinant that renders G
049 alpha(i) sensitive to activation by GIV/girdin is required to promote cell migration. *J Biol Chem*
050 285(17):12765-12777.
- 051 5. Garcia-Marcos M, Ghosh P, & Farquhar MG (2009) GIV is a nonreceptor GEF for Gai with a unique
052 motif that regulates Akt signaling. *Proceedings of the National Academy of Sciences* 106(9):3178-
053 3183.
- 054 6. Garcia-Marcos M, Parag-Sharma K, Marivin A, Maziarz M, Luebbbers A, & Nguyen LT (2020)
055 Optogenetic activation of heterotrimeric G-proteins by LOV2GIVe, a rationally engineered modular
056 protein. *Elife* 9.
- 057 7. Kimple RJ, De Vries L, Tronchere H, Behe CI, Morris RA, Gist Farquhar M, & Siderovski DP (2001)
058 RGS12 and RGS14 GoLoco motifs are G alpha(i) interaction sites with guanine nucleotide
059 dissociation inhibitor Activity. *The Journal of biological chemistry* 276(31):29275-29281.
- 060 8. Stols L, Gu M, Dieckman L, Raffen R, Collart FR, & Donnelly MI (2002) A new vector for high-
061 throughput, ligation-independent cloning encoding a tobacco etch virus protease cleavage site.
062 *Protein Expr Purif* 25(1):8-15.
- 063 9. Cabrita LD, Dai W, & Bottomley SP (2006) A family of E. coli expression vectors for laboratory scale
064 and high throughput soluble protein production. *BMC Biotechnol* 6:12.
- 065 10. Mumby SM & Linder ME (1994) Myristoylation of G-protein alpha subunits. *Methods Enzymol*
066 237:254-268.
- 067 11. Hollins B, Kuravi S, Digby GJ, & Lambert NA (2009) The c-terminus of GRK3 indicates rapid

- 068 dissociation of G protein heterotrimers. *Cell Signal* 21(6):1015-1021.
- 069 12. Qin K, Dong C, Wu G, & Lambert NA (2011) Inactive-state preassembly of G(q)-coupled receptors
070 and G(q) heterotrimers. *Nat Chem Biol* 7(10):740-747.
- 071 13. Masuho I, Ostrovskaya O, Kramer GM, Jones CD, Xie K, & Martemyanov KA (2015) Distinct profiles
072 of functional discrimination among G proteins determine the actions of G protein-coupled receptors.
073 *Sci Signal* 8(405):ra123.
- 074 14. Garcia-Marcos M, Ghosh P, & Farquhar MG (2011) Molecular basis of a novel oncogenic mutation in
075 GNAO1. *Oncogene* 30(23):2691-2696.
- 076 15. Ghosh P, Garcia-Marcos M, Bornheimer SJ, & Farquhar MG (2008) Activation of Galphai3 triggers
077 cell migration via regulation of GIV. *J Cell Biol* 182(2):381-393.
- 078 16. Wedegaertner PB, Chu DH, Wilson PT, Levis MJ, & Bourne HR (1993) Palmitoylation is required for
079 signaling functions and membrane attachment of Gq alpha and Gs alpha. *J Biol Chem* 268(33):25001-
080 25008.
- 081 17. Oner SS, An N, Vural A, Breton B, Bouvier M, Blumer JB, & Lanier SM (2010) Regulation of the
082 AGS3.G{alpha}i signaling complex by a seven-transmembrane span receptor. *The Journal of*
083 *biological chemistry* 285(44):33949-33958.
- 084 18. Ishii K, Hein L, Kobilka B, & Coughlin SR (1993) Kinetics of thrombin receptor cleavage on intact cells.
085 Relation to signaling. *J Biol Chem* 268(13):9780-9786.
- 086 19. Marivin A, Leyme A, Parag-Sharma K, DiGiacomo V, Cheung AY, Nguyen LT, Dominguez I, & Garcia-
087 Marcos M (2016) Dominant-negative Galpha subunits are a mechanism of dysregulated
088 heterotrimeric G protein signaling in human disease. *Sci Signal* 9(423):ra37.
- 089 20. Efendiev R, Samelson BK, Nguyen BT, Phatarpekar PV, Baameur F, Scott JD, & Dessauer CW (2010)
090 AKAP79 interacts with multiple adenylyl cyclase (AC) isoforms and scaffolds AC5 and -6 to alpha-
091 amino-3-hydroxyl-5-methyl-4-isoxazole-propionate (AMPA) receptors. *J Biol Chem* 285(19):14450-
092 14458.
- 093 21. Binkowski BF, Butler BL, Stecha PF, Eggers CT, Otto P, Zimmerman K, Vidugiris G, Wood MG, Encell
094 LP, Fan F, & Wood KV (2011) A luminescent biosensor with increased dynamic range for intracellular
095 cAMP. *ACS chemical biology* 6(11):1193-1197.

- 096 22. Studier FW (2005) Protein production by auto-induction in high density shaking cultures. *Protein*
097 *expression and purification* 41(1):207-234.
- 098 23. Marivin A, Maziarz M, Zhao J, DiGiacomo V, Olmos Calvo I, Mann EA, Ear J, Blanco-Canosa JB,
099 Ross EM, Ghosh P, & Garcia-Marcos M (2020) DAPLE protein inhibits nucleotide exchange on
100 Galphas and Galphaq via the same motif that activates Galphai. *The Journal of biological chemistry*
101 295(8):2270-2284.
- 102 24. Maziarz M, Broselid S, DiGiacomo V, Park JC, Luebbers A, Garcia-Navarrete L, Blanco-Canosa JB,
103 Baillie GS, & Garcia-Marcos M (2018) A biochemical and genetic discovery pipeline identifies
104 PLCdelta4b as a nonreceptor activator of heterotrimeric G-proteins. *The Journal of biological*
105 *chemistry* 293(44):16964-16983.
- 106 25. Leyme A, Marivin A, Maziarz M, DiGiacomo V, Papakonstantinou MP, Patel PP, Blanco-Canosa JB,
107 Walawalkar IA, Rodriguez-Davila G, Dominguez I, & Garcia-Marcos M (2017) Specific inhibition of
108 GPCR-independent G protein signaling by a rationally engineered protein. *Proceedings of the*
109 *National Academy of Sciences of the United States of America* 114(48):E10319-E10328.
- 110 26. Midde KK, Aznar N, Laederich MB, Ma GS, Kunkel MT, Newton AC, & Ghosh P (2015) Multimodular
111 biosensors reveal a novel platform for activation of G proteins by growth factor receptors. *Proceedings*
112 *of the National Academy of Sciences of the United States of America* 112(9):E937-946.
- 113 27. Baell JB (2010) Observations on screening-based research and some concerning trends in the
114 literature. *Future medicinal chemistry* 2(10):1529-1546.
- 115 28. Lagorce D, Sperandio O, Baell JB, Miteva MA, & Villoutreix BO (2015) FAF-Drugs3: a web server for
116 compound property calculation and chemical library design. *Nucleic acids research* 43(W1):W200-
117 207.
- 118 29. Leyme A, Marivin A, Perez-Gutierrez L, Nguyen LT, & Garcia-Marcos M (2015) Integrins activate
119 trimeric G proteins via the nonreceptor protein GIV/Girdin. *The Journal of cell biology* 210(7):1165-
120 1184.
- 121 30. Maziarz M, Park JC, Leyme A, Marivin A, Garcia-Lopez A, Patel PP, & Garcia-Marcos M (2020)
122 Revealing the Activity of Trimeric G-proteins in Live Cells with a Versatile Biosensor Design. *Cell*
123 182(3):770-785 e716.
- 124 31. Wishart DS, Bigam CG, Holm A, Hodges RS, & Sykes BD (1995) (1)H, (13)C and (15)N random coil

- 125 NMR chemical shifts of the common amino acids. I. Investigations of nearest-neighbor effects. *Journal*
126 *of biomolecular NMR* 5(3):332.
- 127 32. Lee W, Tonelli M, & Markley JL (2015) NMRFAM-SPARKY: enhanced software for biomolecular NMR
128 spectroscopy. *Bioinformatics* 31(8):1325-1327.
- 129 33. Mase Y, Yokogawa M, Osawa M, & Shimada I (2014) Backbone resonance assignments for G protein
130 alpha(i3) subunit in the GDP-bound state. *Biomolecular NMR assignments* 8(2):237-241.
- 131 34. San Sebastian E, et al. (2013) Design, synthesis, and functional evaluation of leukocyte function
132 associated antigen-1 antagonists in early and late stages of cancer development. *Journal of medicinal*
133 *chemistry* 56(3):735-747.
- 134 35. Palacios A, Garcia P, Padro D, Lopez-Hernandez E, Martin I, & Blanco FJ (2006) Solution structure
135 and NMR characterization of the binding to methylated histone tails of the plant homeodomain finger
136 of the tumour suppressor ING4. *FEBS letters* 580(30):6903-6908.
- 137 36. Cer RZ, Mudunuri U, Stephens R, & Lebeda FJ (2009) IC50-to-Ki: a web-based tool for converting
138 IC50 to Ki values for inhibitors of enzyme activity and ligand binding. *Nucleic acids research* 37(Web
139 Server issue):W441-445.
- 140 37. Abagyan R, Totrov M, & Kuznetsov D (1994) Icm - a New Method for Protein Modeling and Design -
141 Applications to Docking and Structure Prediction from the Distorted Native Conformation. *J Comput*
142 *Chem* 15(5):488-506.
- 143 38. Totrov M & Abagyan R (1997) Flexible protein-ligand docking by global energy optimization in internal
144 coordinates. *Proteins Suppl* 1:215-220.
- 145 39. Halgren TA & Nachbar RB (1996) Merck molecular force field .4. Conformational energies and
146 geometries for MMFF94. *J Comput Chem* 17(5-6):587-615.
- 147 40. Nemethy G, Gibson KD, Palmer KA, Yoon CN, Paterlini G, Zagari A, Rumsey S, & Scheraga HA (1992)
148 Energy Parameters in Polypeptides .10. Improved Geometrical Parameters and Nonbonded
149 Interactions for Use in the Ecepp/3 Algorithm, with Application to Proline-Containing Peptides. *J Phys*
150 *Chem-Us* 96(15):6472-6484.
- 151 41. Garcia-Marcos M, Kietrsunthorn PS, Wang H, Ghosh P, & Farquhar MG (2011) G Protein binding
152 sites on Calnuc (nucleobindin 1) and NUCB2 (nucleobindin 2) define a new class of G(alpha)-
153 regulatory motifs. *J Biol Chem* 286(32):28138-28149.

- 154 42. Garcia-Marcos M (2021) Complementary biosensors reveal different G-protein signaling modes
155 triggered by GPCRs and non-receptor activators. *eLife* 10.
- 156 43. Freissmuth M, Boehm S, Beindl W, Nickel P, Ijzerman AP, Hohenegger M, & Nanoff C (1996) Suramin
157 analogues as subtype-selective G protein inhibitors. *Molecular pharmacology* 49(4):602-611.
- 158 44. Parag-Sharma K, Leyme A, DiGiacomo V, Marivin A, Broselid S, & Garcia-Marcos M (2016)
159 Membrane Recruitment of the Non-receptor Protein GIV/Girdin (Galpha-interacting, Vesicle-
160 associated Protein/Girdin) Is Sufficient for Activating Heterotrimeric G Protein Signaling. *J Biol Chem*
161 291(53):27098-27111.
- 162 45. Debnath J, Muthuswamy SK, & Brugge JS (2003) Morphogenesis and oncogenesis of MCF-10A
163 mammary epithelial acini grown in three-dimensional basement membrane cultures. *Methods*
164 30(3):256-268.
- 165 46. Muller RE, Klein KR, Hutsell SQ, Siderovski DP, & Kimple AJ (2010) A homogeneous method to
166 measure nucleotide exchange by alpha-subunits of heterotrimeric G-proteins using fluorescence
167 polarization. *Assay and drug development technologies* 8(5):621-624.
- 168
- 169